Journal Pre-proof

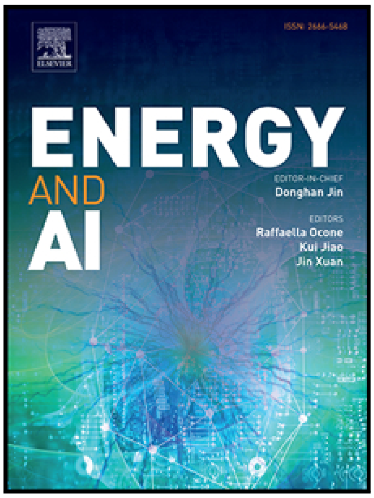

Two-stage capacity optimization approach of multi-energy system considering its optimal operation

X.J. Luo , Lukumon O. Oyedele , Olugbenga O. Akinade , Anuoluwapo O. Ajayi

PII: S2666-5468(20)30005-7
DOI: https://doi.org/10.1016/j.egyai.2020.100005
Reference: EGYAI 100005

To appear in: *Energy and AI*

Received date: 10 February 2020
Revised date: 21 March 2020
Accepted date: 5 April 2020

Please cite this article as: X.J. Luo , Lukumon O. Oyedele , Olugbenga O. Akinade , Anuoluwapo O. Ajayi , Two-stage capacity optimization approach of multi-energy system considering its optimal operation, *Energy and AI* (2020), doi: https://doi.org/10.1016/j.egyai.2020.100005

HIghlights

- A two-stage capacity optimization approach is proposed for MES with its optimal operating schedule taken into account;
- Two stages of optimization are interrelated to determine the optimal design and operating capacities of energy devices simultaneously and effectively;
- The variable efficiency of energy devices due to loading and weather conditions are considered;
- The key energy devices involve biomass-based PGU, heat exchanger, absorption chiller, electric chiller, biomass boiler, BIPV and PVT;
- Different GA parameters are adopted to guarantee the global optimal results being identified.

Two-stage capacity optimization approach of multi-energy system considering its optimal operation

X.J. Luo, Lukumon O. Oyedele*, Olugbenga O. Akinade and Anuoluwapo O. Ajayi

Big Data Enterprise and Artificial Intelligence Laboratory (Big-DEAL)
University of the West of England (UWE), Frenchay Campus, Bristol, United Kingdom
*Corresponding author: L.Oyedele@uwe.ac.uk

Abstract

With the depletion of fossil fuel and climate change, multi-energy systems have attracted widespread attention in buildings. Multi-energy systems, fuelled by renewable energy, including solar and biomass energy, are gaining increasing adoption in commercial buildings. Most of previous capacity design approaches are formulated based upon conventional operating schedules, which result in inappropriate design capacities and ineffective operating schedules of the multi-energy system. Therefore, a two-stage capacity optimization approach is proposed for the multi-energy system with its optimal operating schedule taken into consideration. To demonstrate the effectiveness of the proposed capacity optimization approach, it is tested on a renewable energy fuelled multi-energy system in a commercial building. The primary energy devices of the multi-energy system consist of biomass gasification-based power generation unit, heat recovery unit, heat exchanger, absorption chiller, electric chiller, biomass boiler, building integrated photovoltaic and photovoltaic thermal hybrid solar collector. The variable efficiency owing to weather condition and part-load operation is also considered. Genetic algorithm is adopted to determine the optimal design capacity and operating capacity of energy devices for the first-stage and second-stage optimization, respectively. The two optimization stages are interrelated; thus, the optimal design and operation of the multi-energy system can be obtained simultaneously and effectively. With the adoption of the proposed novel capacity optimization approach, there is a 14% reduction of year-round biomass consumption compared to one with the conventional capacity design approach.

Keywords: Multi-energy system; Renewable energy; Biomass; Genetic algorithm; Capacity design; Optimization.

1. Introduction

Energy crisis and global warming are becoming urgent issues in the current world [1, 2]. The renewable energy such as solar, biomass and wind has been playing a significant role in energy conservation and emission reduction. As an effective approach to utilize renewable energy, multi-energy systems (MES) have attracted attention worldwide recently. In general, MES can be regarded as a multi-input-multi-output energy system, which can utilize multiple types of energy sources and which is capable of simultaneously providing heating, cooling and electrical energy to buildings. Therefore, it has the advantages of high energy efficiency, low carbon emission and high operating reliability [3]. However, it is difficult to determine the optimal configuration of the MES owing to its highly inter-coupled characteristics [4]. It is mainly owing to the fact that the same type of energy demand (heating, cooling or electrical energy) can be generated by various energy devices, and the same energy device can generate various types of energy production. It is difficult to determine the design capacity of a single energy device according to one type of energy demand.

1.1 Related works

In order to determine the optimal configuration and design capacity of energy devices in the MES, various optimization algorithms were adopted, including genetic algorithm, Recursive quadratic approximation algorithm and dynamic programming. Patrizia *et al.* [5] proposed an evolutionary algorithm-based multi-objective optimization approach to select the appropriate capacity of each energy device thus identify the optimal MES layout. At the capacity design stage, the MES was assumed to operate at the electric equivalent demand following strategy. In other words, the optimal design capacity was determined on the assumption that the system was operated to cover the basic building electricity load and the electricity needed for the electric chiller. Wang *et al.* [6] proposed a capacity optimization approach for the solar-assisted MES based on the exergo-economic analysis. At the capacity design stage, the MES was assumed to operate according to the following electricity strategy. Namely, the optimal design capacity was obtained on the assumption that the MES was operated to cover the basic building electricity load. Luo *et al.* [7] proposed a multi-objective nonlinear optimization model for the device capacity of the MES with the economic, environmental and energy objectives accounted simultaneously. The MES was operated according to the pre-set operating schedule based on its load demand and renewable energy production. Pan *et al.* [8] proposed a planning strategy to determine the optimal capacity of the energy devices in the MES thus to manage its heating, cooling and electrical energy supply to end-users in the building. The optimization objective of the planning strategy was to minimize the annual consumption expense. Wei *et al.* [9] proposed multi-objective interval optimization model to solve the sizing problem of the MES thus to reduce the primary energy consumption, operating cost and carbon emission. However, the conventional formulation based operating strategy was adopted in the proposed MES. Rong *et al.* [10] adopted the multi-population genetic algorithm to optimize the capacity design and operating schedule of a hybrid district heating and cooling system to minimize the life cycle cost. A critical value was also chosen by the proposed optimization approach to determine whether to operate the gas engine. Gholamhossein *et al.* [11] proposed a multi-objective optimization approach to determine the nominal capacity of energy devices of a MES according to its exergetic efficiency, total levelized cost rate as well as the cost rate of the environment. However, it was assumed that the MES was constantly operated a full-load at the design stage. Li *et al.* [12] proposed a multi-criteria optimization for the biomass-fuelled MES based on life-cycle assessment. The criteria comprise the primary energy saving ratio, total cost saving ratio and carbon emission reduction ratio. The effects of following electrical load and following thermal load were compared at the design stage. Lin *et al.* [13] proposed a genetic algorithm-based multi-objective optimization approach to determine the optimal design capacity of the power generation unit and absorption chiller. The optimization objectives included primary energy saving, life cycle cost reduction and carbon dioxide emission reduction. At the design stage, the MES was assumed to be operated based on the following thermal load strategy. Bahlawan *et al.* [14] proposed a dynamic programming optimization method to determine the design capacities of energy devices in the MES. The optimization problem was carried out to minimize primary energy consumption over the simulation period. However, the cogeneration unit was assumed to operate at full-load or be turned off at the design stage.

1.2 Research gaps and contribution

The energy devices adopted in the MES, the optimization variables, optimization objectives, optimization algorithms and operating strategy of the above-mentioned studies are summarized in Table 1. In most of the studies, the design capacity of energy devices were chosen as the optimization variables while primary energy consumption, operating cost and carbon emission were set as optimization objectives. However, the following deficits were identified in the literature review:

- Conventional operating strategies, such as constantly full-load operation, following electric load, following thermal load, following equivalent electric load or formulation-based operating strategy, were generally adopted at the design stage. The conventional strategy itself would result in excessive energy production in most of the load demand situations;
- The MES was not sufficient enough in energy-saving: for example, energy storages, which could shift peak load demand, were not adopted in [5, 9-13]. In addition, electric chiller, which has higher efficiency than absorption chiller, was not adopted in [6-8, 10, 14];
- In some of the previous research works, the key energy devices, including power generation unit, absorption chiller and electric chiller, were operated at constant efficiency. However, the efficiency of most practical devices would be variable under different operating and weather conditions;
- As for the optimization algorithm, none of the existing research mentioned how to choose the parameters of each algorithm. Therefore, they may result in local optimal rather than the global optimum.

Given the above-discussed research gaps, this paper aims to propose an effective capacity optimization approach which has the following characteristics:

Table 1. Summary of reference

Ref	Optimization variables	Energy devices	Operating strategy	Optimization objectives	Optimization algorithms
5	PV coverage ratio and design capacity of PGU	PGU, absorption chiller electric chiller, boiler, PV panel and solar thermal collector with constant efficiency	Following equivalent electric load	Energy, environment and economic	Evolutionary algorithm with population of 500 and generation of 200
6	PV coverage ratio, supplement heat ratio	PV/T collector, ICE, absorption heat pump with cooling tower, HS and heat exchanger.	Following electric load	Exergo-economic	Recursive quadratic approximation algorithm
7	Design capacity of energy devices	PV panel, air source heat pump, ground source heat pump, boiler, solar thermal collector, ES and HS with constant efficiency	Formulations based operating strategy	Energy, environment and economic	NSGAII
8	Design capacity of energy devices	PV panel, Gas turbine, boiler, HX, absorption chiller and HS with constant efficiency	Integrated demand response program	Annual capital and operating cost	YALMIP for MILP
9	Design capacity of energy devices	Wind turbine, solar thermal collector, electric boiler, gas boiler, absorption chiller and electric chiller with constant efficiency	Formulations based heating mode and cooling mode	Life cycle cost	Multi-objective group search optimization with adaptive covariance and chaotic search
10	Thermal capacity of gas engine, ratio of heating/cooling by GSHP, critical value	Gas engine, ground source heat pump, boiler, absorption chiller and heat exchanger	Heating mode and cooling mode with a critical value to judge whether operate the gas engine	primary energy saving, co2 emission reduction, annual total cost saving	Multi-population genetic algorithm
11	Design capacity of micro turbine and absorption chiller	Micro-turbine, auxiliary boiler, absorption chiller and electric chiller with constant efficiency	Full load operation	Exergertic efficiency, total levelized cost rate of the system, cost rate of environmental	GA, population size=500, maximum generation=300, crossover=70%, mutation 1%
12	Design capacity of PGU, type of biomass stock	Biomass based ICE, absorption chiller, electric chiller and heat exchanger	Following electric load Following heat load	Energy, environment and economic	Technique for Order of Preference by Similarity to Ideal Solution
13	Design capacity of PGU and chiller	PGU, electric chiller, absorption chiller and boiler	9 mode operating strategy	Energy, environment and economic	GA, population size=100, maximum generation=100, crossover=0.8, mutation=0.4
14	Design capacity of energy devices	Solar thermal collector, PV, auxiliary boiler, heat pumps, cogeneration unit and hot water storage	Cogeneration unit fully on or off	Minimizing primary energy consumption	Dynamic programming

- The design capacity of energy devices and the optimal operating schedules of the MES are determined simultaneously and interrelatedly. In other words, the design configuration of MES is determined based on its optimal operating schedules thus to exploit the potential of MES fully;
- The proposed capacity optimization approach is adopted on a comprehensive MES, which involves building integrated photovoltaic (BIPV), photovoltaic thermal hybrid solar collector (PVT), biomass gasification-based power generation unit (PGU), absorption chiller (AC), electric chiller (EC), heat exchanger (HX), biomass boiler and various energy storages;
- The variable efficiency of BIPV, PVT, PGU, AC and EC at different loading and weather conditions are considered to represent its practical performance;
- The parameters of genetic algorithm, including population size, retain percentage, crossover percentage and mutation percentage, are chosen by the numeration method to avoid possible local optimum results.

The rest of this paper is organized as follows: Section 2 provides an overview of the MES dynamic model and the representative commercial building; Section 3 illustrates the proposed two-stage capacity optimization approach; The results and discussion are outlined in Section 4; Section 5 draws the conclusion of the paper and points out directions of future study.

2. Development of MES dynamic model and representative commercial building

To satisfy the cooling, heating and electrical energy of the commercial building, a comprehensive renewable energy fuelled MES is designed.

2.1 System design

The schematic design of the MES is shown in Fig. 1. Solar energy and biomass are the two renewable energy sources adopted to drive the whole MES system.

- For building electricity supply, the solid biomass is gasified in the gasification system and supplied to the internal combustion engine for electricity production. The biomass-based internal combustion engine can also be called power generation unit (PGU). Meanwhile, solar energy is converted into electricity through BIPV and PVT. In addition, electricity storage is adopted for electricity load shifting purposes.
- For building cooling supply, the heating energy recovered from the PGU can be adopted to drive the absorption chiller. Meanwhile, the electricity generated by the PGU can be adopted to drive the electric chiller. In addition, cold storage is adopted for heating load shifting purposes.
- For building heating supply, the exhaust heat from the power generation unit is recovered through

heat recovery system and delivered to the heat exchanger for heating supply. Moreover, solar energy is converted to thermal energy through PVT. Meanwhile, biomass is also supplied to the biomass boiler for heating purposes. In addition, heat storage is adopted for heating load shifting purposes.

Therefore, the MES can be regarded as a multi-supply-multi-demand system, solar energy and biomass are the two major renewable sources, while electricity, cooling and heating are the three types of energy demands from the building.

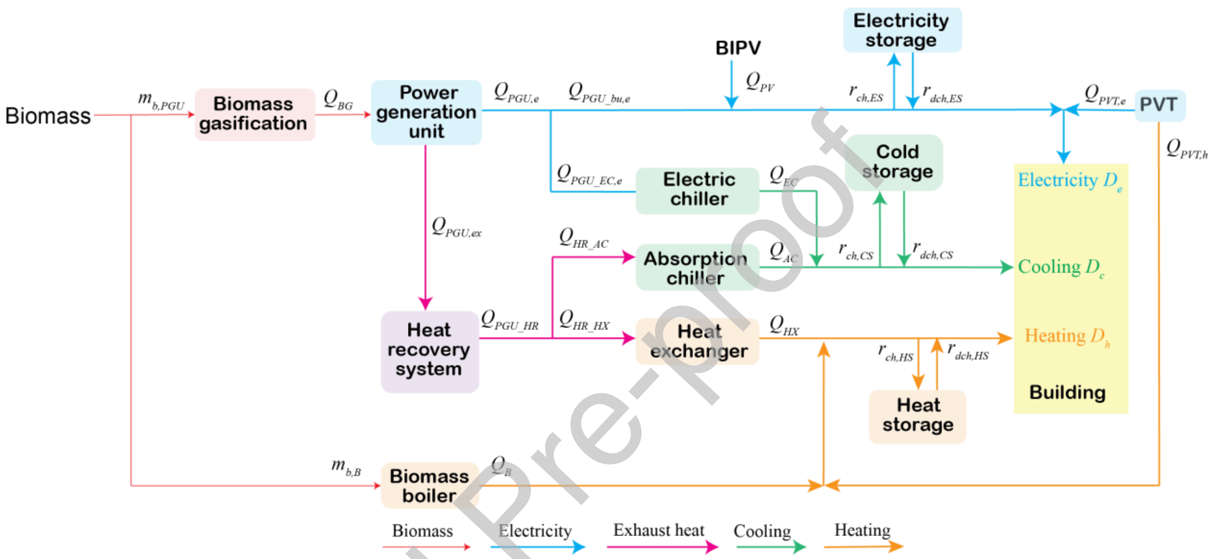

Fig. 1. Schematic diagram of the MES.

The energy devices in the MES include biomass gasification system, biomass-based PGU, BIPV, PVT, absorption chiller, electric chiller, biomass boiler, heat exchanger, electricity storage, cold storage and heat storage. The thermodynamic models of each energy device are summarized in Table 2. To make the system simulation result closer to the practical operation, the effects of weather and loading conditions on the efficiency of BIPV, PVT, biomass-based PGU, absorption chiller and electric chiller are considered. For BIPV and PVT, the validated model in [15] is adopted, in which the thermal and electrical efficiency is affected by the actual outdoor air dry-bulb temperature and solar radiation. For biomass-based PGU, the validated model in [12] is adopted. For absorption chiller and electric chiller, their coefficient of performance (*COP*) are dependent on cooling water inlet temperature and the part-load ratio [4, 16]. For heat and cold storages, the hot water tank and chilled water tank are adopted, respectively; For electricity storage, the Lithium-Ion battery is adopted [17]. The design parameters of the energy storages, along with the heat recovery system, biomass boiler and heat exchanger, are summarized in Table 3.

Table 2. Thermodynamic model of the MES.

Biomass gasification system	$Q_{BG} = m_{b,PGU} LHV_{bio} \eta_{BG}$
Power generation unit	$Q_{PGU,e} = \eta_{PGU,e} Q_{BG}$ $Q_{PGU,ex} = \eta_{PGU,ex} Q_{BG}$ $Q_{PGU\_HR} = \eta_{HR} Q_{PGU,ex}$
BIPV	$Q_{BIPV} = \varphi A_{BIPV} \alpha_{BIPV} \eta_{BIPV}$ $\eta_{BIPV} = \eta_{BIPV,n}[1+\varepsilon_T(T_{BIPV}-T_{ref})][1+\varepsilon_\varphi(\varphi_{BIPV}-\varphi_{ref})]$
PVT	$Q_{PVT,e} = \eta_{PVT,e} \times \varphi \times A_{PVT}$ $Q_{PVT,h} = \eta_{PVT,h} \times \varphi \times A_{PVT}$ $\eta_{PVT,e} = \eta_{PVT,e}[1+\varepsilon_T(T_{PVT}-T_{ref})][1+\varepsilon_\varphi(\varphi_{PVT}-\varphi_{ref})]$ $\eta_{PVT,h} = \eta_{PVT,h}[1+\varepsilon_T(T_{PVT}-T_{ref})][1+\varepsilon_\varphi(\varphi_{PVT}-\varphi_{ref})]$
Absorption chiller	$Q_{AC} = Q_{HR\_AC} COP_{AC}$
Electric chiller	$Q_{EC} = Q_{PGU\_EC} COP_{EC}$
Biomass boiler	$Q_B = \eta_B m_{b,B} LHV_{bio}$
Heat exchanger	$Q_{HX} = \eta_{HX} Q_{HR\_HX}$
Electricity storage	$E_{ES,j+1} = E_{ES,j} + r_{ch,ES}\eta_{ch,ES} - r_{dch,ES}/\eta_{dch,ES}$
Cold storage	$E_{CS,j+1} = E_{CS,j} + r_{ch,CS}\eta_{ch,CS} - r_{dch,CS}/\eta_{dch,CS}$
Heat storage	$E_{HS,j+1} = E_{HS,j} + r_{ch,HS}\eta_{ch,HS} - r_{dch,HS}/\eta_{dch,HS}$

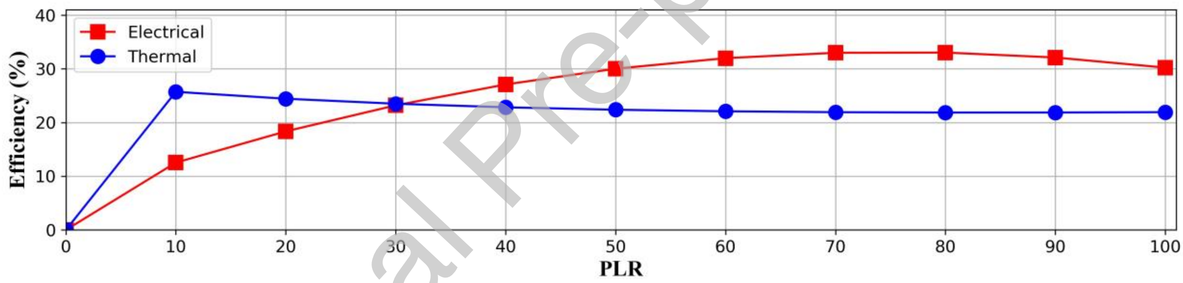

(a) Biomass-based PGU

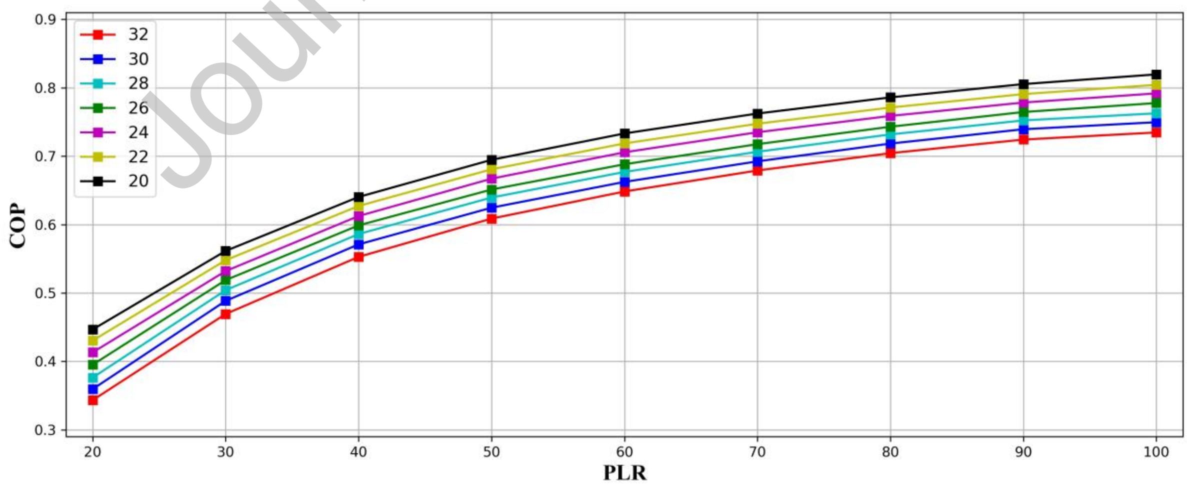

(b) Absorption chiller

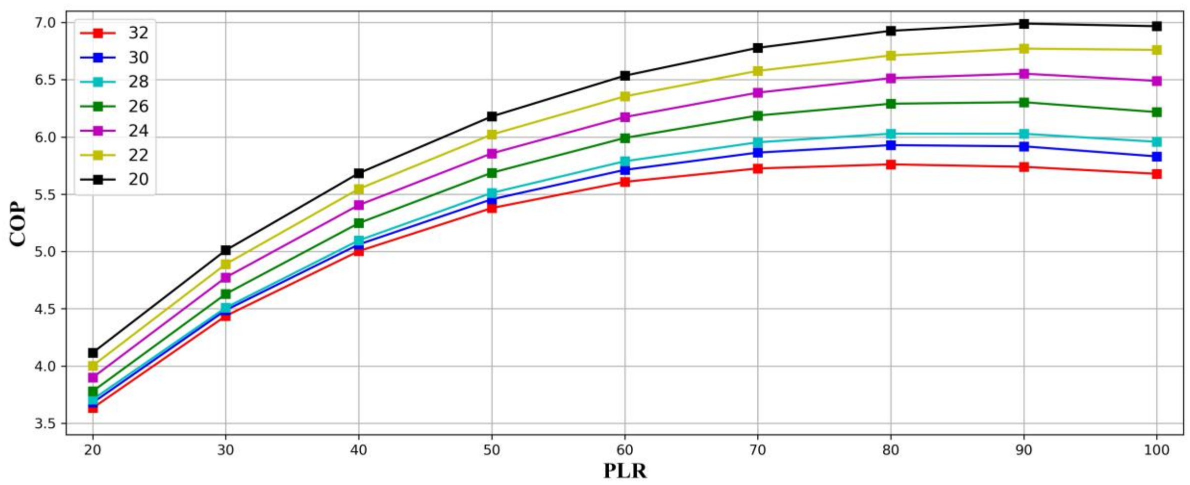

(c) Electric chiller

Fig. 2. Efficiency and COP of biomass-based PGU, absorption chiller and electric chiller

Table 3. Design parameters of the energy devices.

	Design parameter	Value
BIPV/PVT [15]	Absorption of PV surface	0.8
	Emissivity of PV surface	0.9
	Substrate resistance (h m^2 K/kJ)	0.01
	Channel emissivity	0.9
	Back resistance (h m^2 K/kJ)	1.0
	Channel height (m)	0.0508
	Reference PV efficiency	0.12
	Reference temperature	25
	Reference radiation (kJ /h m^2)	3600
	Efficiency modifier temperature	-0.005
	Efficiency modifier radiation (kJ /h m^2)	0.000025
Energy storages [4, 16, 17]	Charge efficiency of CS (%)	90
	Discharge efficiency of CS (%)	90
	Charge efficiency of HS (%)	90
	Discharge efficiency of HS (%)	90
	Charge efficiency of ES (%)	95
	Discharge efficiency of ES (%)	85
Heat recovery system [16]	Efficiency (%)	90
Heat exchanger [16]	Efficiency (%)	90
Biomass boiler [18]	Efficiency (%)	80

2.2 Building information

The typical office building in the United Kingdom as detailed in [19, 20] is adopted to identify the representative year-round heating, cooling and electricity demands of commercial buildings. The 3D drawing and floor plan of the reference 4-storey commercial building are presented in Figs. 3 and 4, respectively. The floor size is 32 × 16 m^2 with the floor-to-ceiling distance of 3.5m. The floor plan is identical on each floor and is divided into three zones: zone 1A and zone 1B are office rooms while zone 2 is the corridor. The windows are distributed on the north, west and east-sided walls, with the window-to-wall-ratio of 1:2.

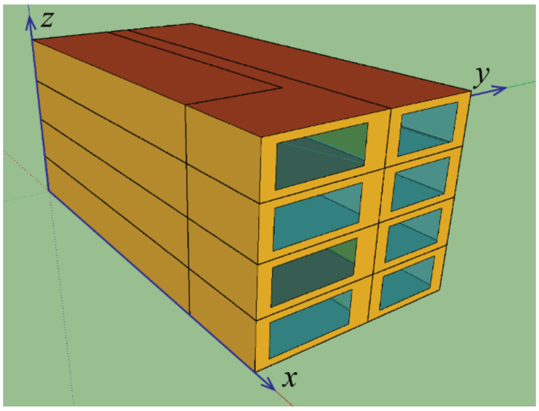

Fig. 3. 3D drawing of the representative commercial building.

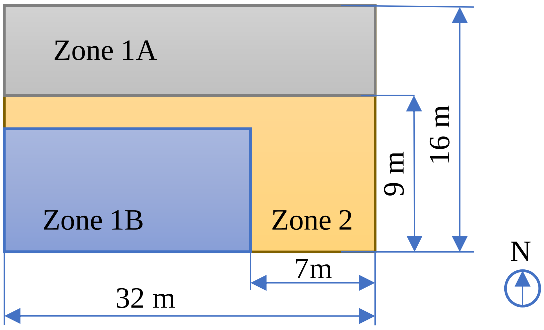

Fig. 4. Floor layout of the representative commercial building.

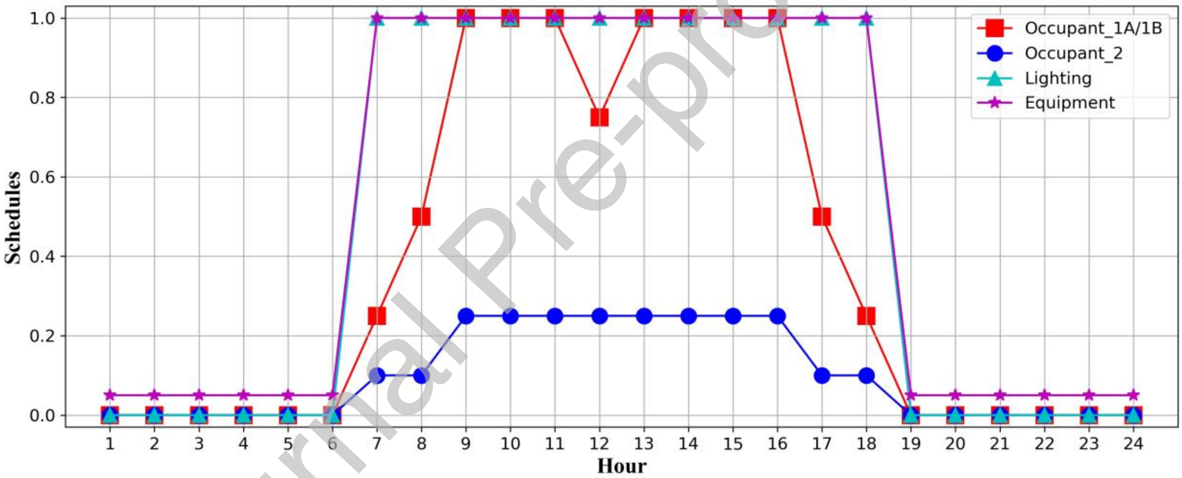

Fig. 5. Operating schedules of the office building on weekdays.

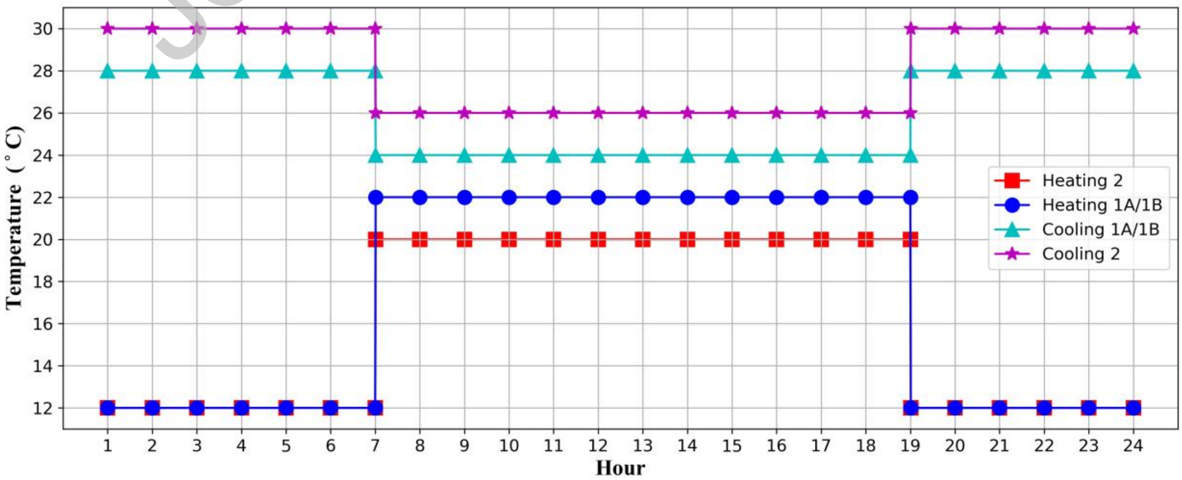

Fig. 6. Temperature setpoints of heating and cooling on the weekdays.

Table 4. U-values of building surfaces.

Building element	External wall	Top roof	Ground floor	Window
U-values (W/m^2 K)	1.517	0.14	0.14	1.51

Table 5. Indoor design conditions of the office building.

Indoor design feature		Value
Zone floor area per person (m²/person)	Cellular offices (1A/1B)	14
	Common areas (2)	8
Lighting power intensity (W/m^2)	Cellular offices (1A/1B)	12
	Common areas (2)	3.4
Equipment heat gains (W/m^2)	Cellular offices (1A/1B)	10
	Common areas (2)	2
Fresh air requirement (L/s/person)		10
Sensible heat gain of occupant (W/person)		75
Latent heat gain of occupant (W/person)		75
Air change per hour through infiltration		0.3

On weekdays, the pre-set operating schedules of occupant, lighting and office equipment during the weekdays are presented in Fig. 5, while the temperature set-points of heating and cooling are shown in Fig. 6. On weekends, the operating schedules and temperature setpoints are equal to those at non-working hours (i.e. 1-6 h, and 19-24 h) on weekdays. The heat transfer coefficients of building surfaces and indoor design conditions are summarized in Tables 4 and 5, respectively.

The typical weather data from London is adopted to explore the energy performance of the developed commercial building. The dry-bulb temperature, relative humidity and solar radiation are depicted in Fig. 7. The outdoor air dry-bulb temperature reaches about 24~29 °C in summer, while drops to around -3~-7 °C in winter. The relative humidity varies from about 40% to 100% during the year. Moreover, the solar radiation reached its peak at about 3000 kJ·h^{-1}·m^{-2} during the summertime.

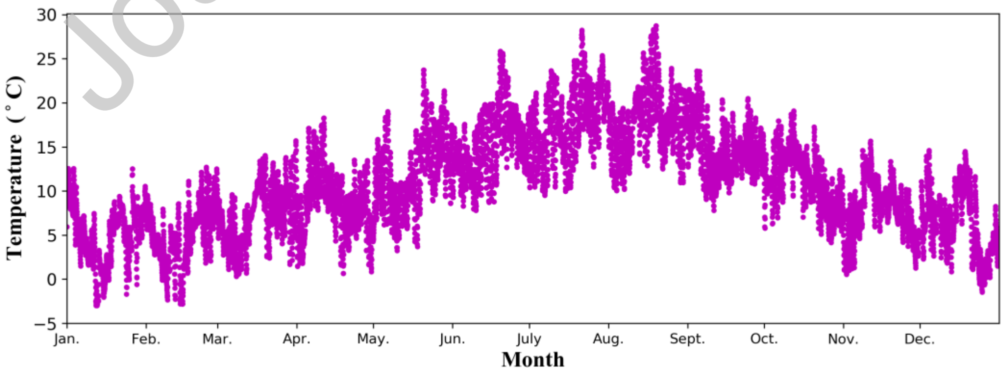

(a) Dry-bulb temperature

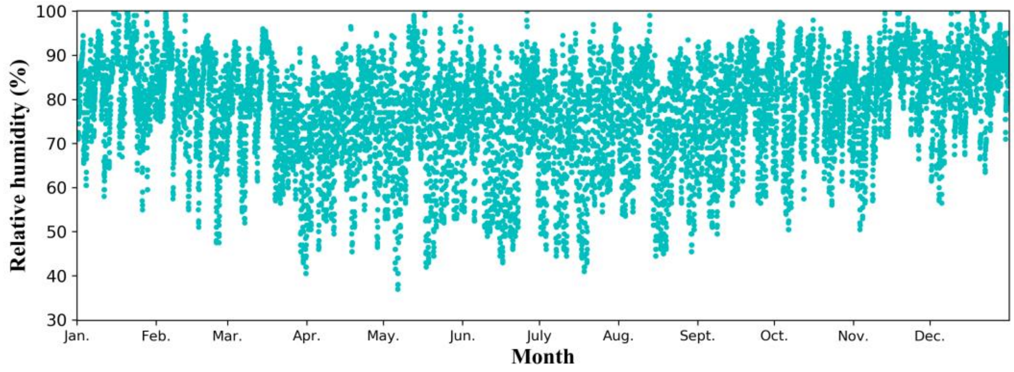

(b) Relative humidity

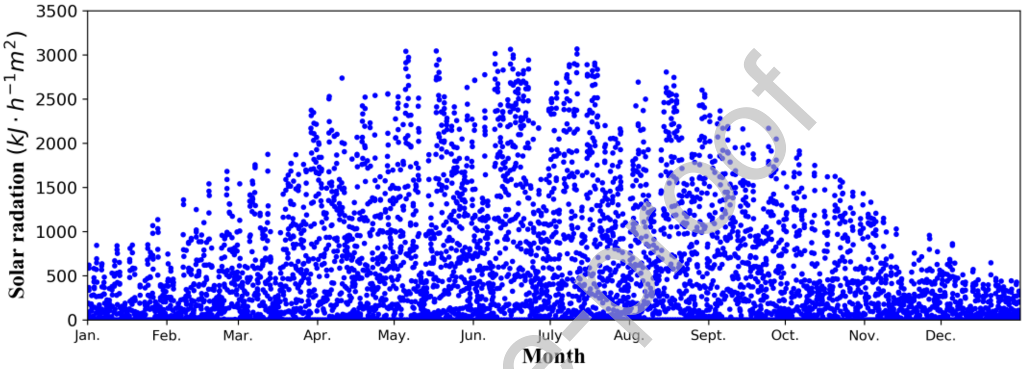

(c) Solar radiation

Fig. 7. London weather data during the Typical Meteorological Year.

Due to the year-round changing weather condition, transient simulation platform TRNSYS 18 [21] and the validated thermal building model Type 56 is adopted to obtain the annual profile of hourly cooling, heating and electrical energy demands. The year-round basic heating, cooling and basic electricity demands are summarized in Fig. 8.

From January to middle May, and October to December, the basic heating energy demand $D_{h,b}$ stands for the thermal energy for both space heating and hot drinking water. Due to the relatively high outdoor air dry-bulb temperature, from middle May towards the end of September, space heating is not needed while thermal energy is only used for hot drinking water. The highest heating energy demand reaches 464594 kJ/h at the second week of January.

The cooling energy demand D_c exists from middle May towards the end of October owing to the relatively high outdoor air dry-bulb temperature and solar radiation, while its peak happens at the middle of August with the value of 306824 kJ/h.

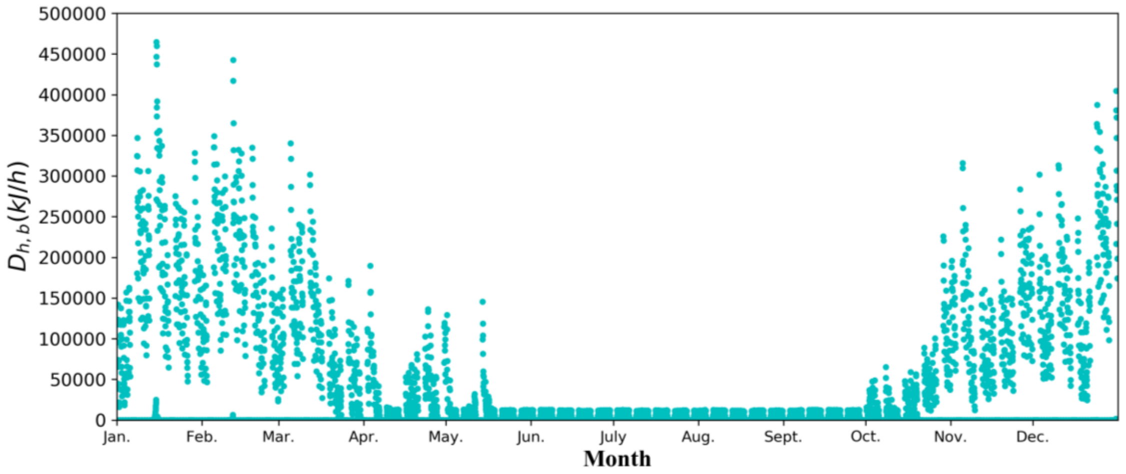

(a) Heating

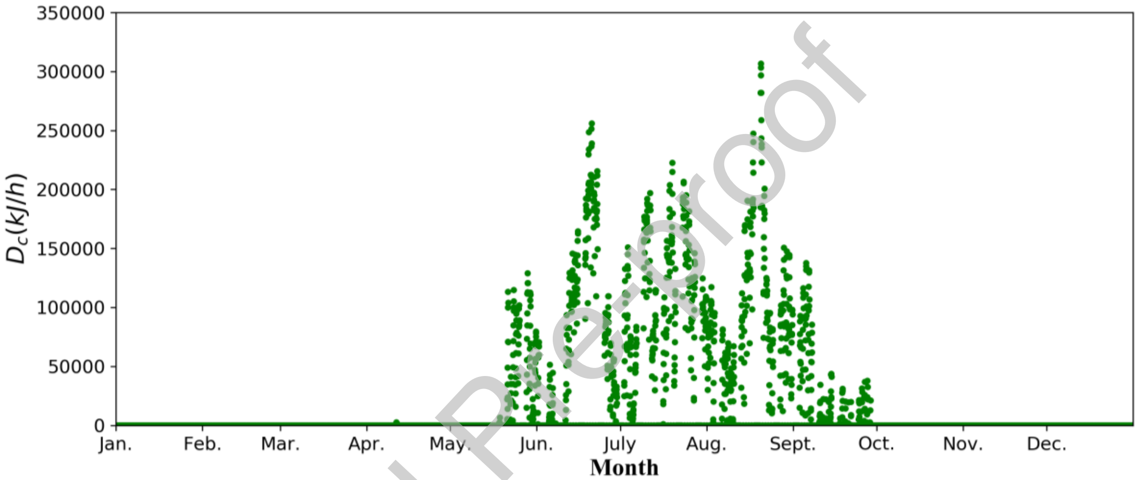

(b) Cooling

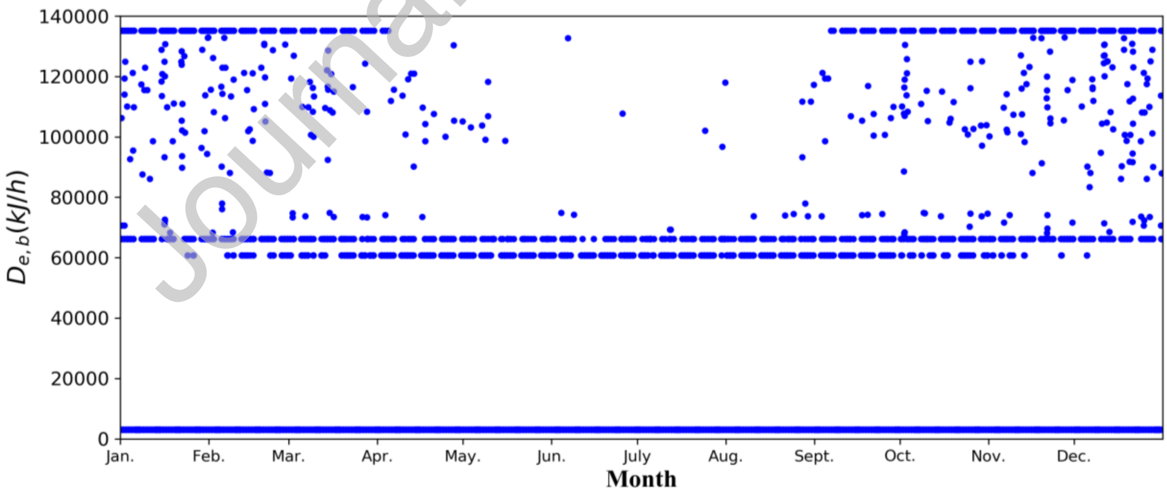

(c) Electrical

Fig. 8. Year-round cooling, heating and electrical energy demand.

The basic electrical energy demand $D_{e,b}$ indicates the electricity used for lighting and office equipment. During non-office hours during the weekday and weekends, the essential office equipment was kept on, thus it results in low but constant electricity consumption during that period (as shown on the bottoming blue dots). Moreover, based on the daylight value, artificial lighting control is adopted to reduce electrical energy consumption. Therefore, three typical values can be identified for electricity consumption, while it varies owing to the variation of daylight. The peak electrical energy demand is 135190 kJ/h when both lighting and office equipment is operated at its peak value.

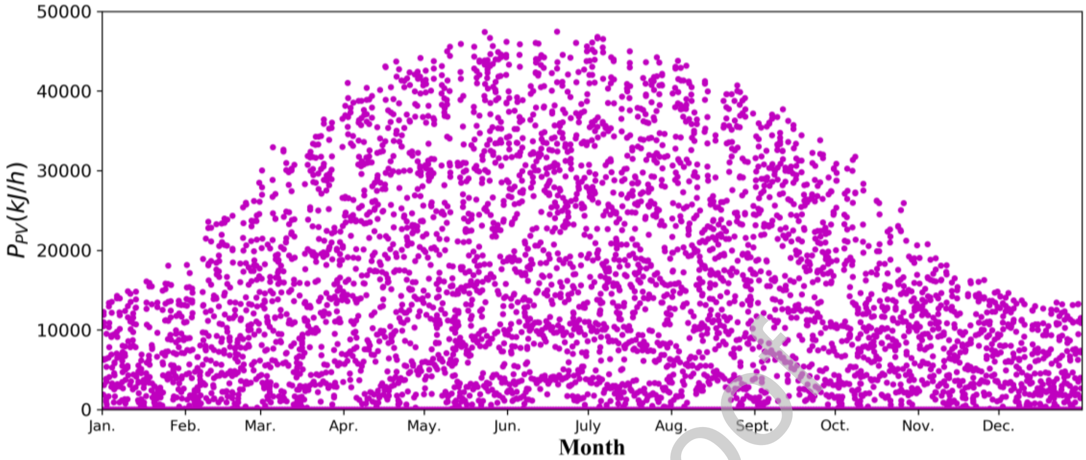

(a) Electrical energy production from BIPV

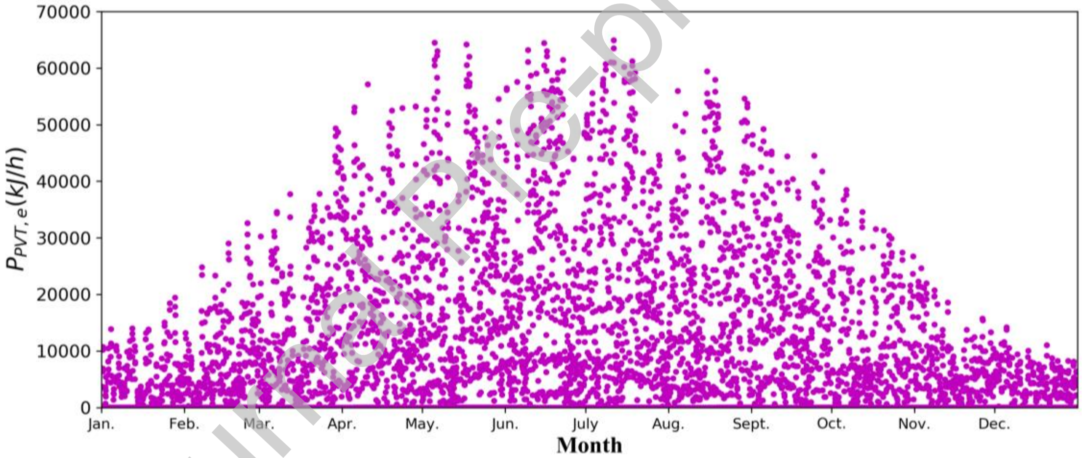

(b) Electrical energy production from PVT

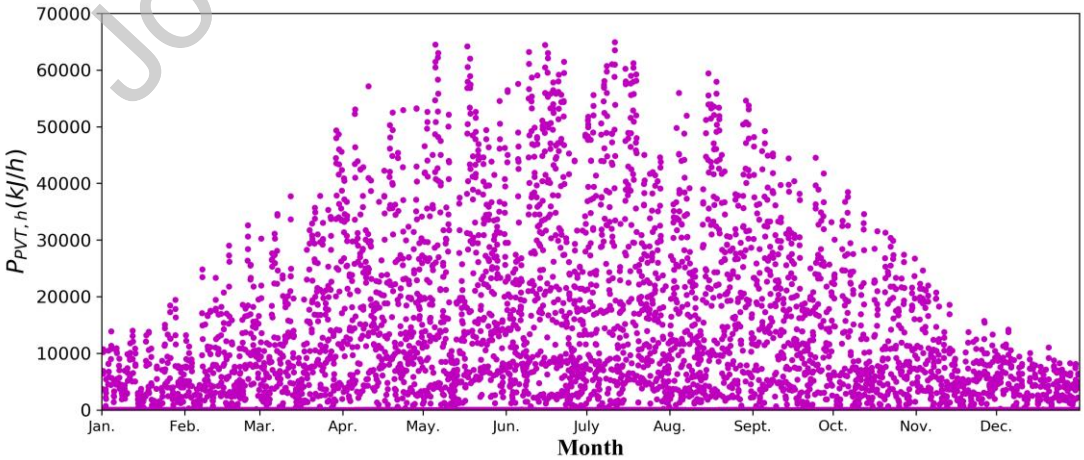

(c) Thermal energy from PVT

Fig. 9. Electrical and thermal energy production from solar power.

To fully utilize the solar energy, BIPV panels are equipped on the whole area south-faced wall, while PVT panels are installed on the entire roof of the building. The electrical energy production from BIPV and PVT panels as well as the thermal energy production from PVT panels are dependent on the outdoor air dry-bulb temperature and solar radiation, as shown in Fig. 9. As a result, the electricity production from BIPV and PVT panels as well as the thermal energy from PVT are relatively high during May and August.

3. Two-stage capacity optimization approach

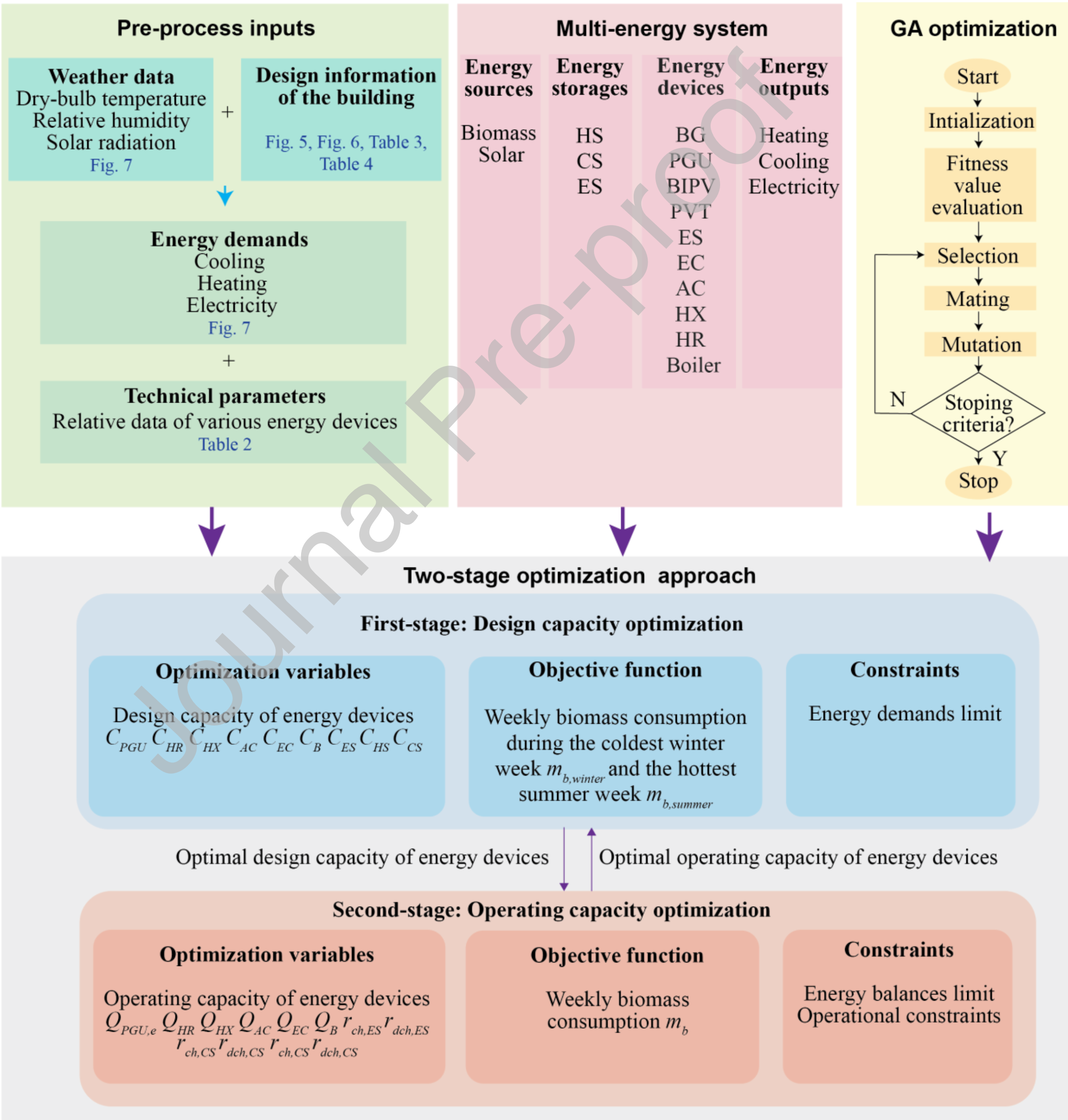

Fig. 10. Schematic diagram of the proposed two-stage optimization approach.

The aim of the proposed optimization approach is to determine the optimal design capacity of each energy device involved in the MES. Since the optimal design capacity of each energy device is depended on its actual operating schedule, the optimal operating schedule is taken into account in the proposed two-stage capacity optimization approach. In other words, the optimal design capacity and operating capacity of the MES are obtained by performing two interrelated stages of optimization: the resulted optimal design capacity from the first-stage optimization is used as operational constraints in the second-stage optimization, while the resulted optimal operating capacity from the second-stage is adopted in determining objective function in the first-stage optimization. The schematic diagram of the proposed two-stage capacity optimization approach is illustrated in Fig. 10. Since biomass is the only primary energy sources consumed in the MES, the primary energy consumption, economic cost and carbon emission all depend on biomass consumption. Therefore, it is regarded as the objective function in both the first-stage and second-stage optimization.

3.1 First-stage optimization

The objective of the first-stage optimization is to determine the optimal design capacity of each energy device in the MES, based on the optimal operating capacity determined in the second-stage optimization.

3.1.1 Design variables

In the first-stage optimization, the design capacities of power generation unit $C_{PGU,e}$, biomass boiler C_B, absorption chiller C_{AC}, electric chiller C_{EC}, electricity storage C_{ES}, heating storage C_{HS} and cooling storage C_{CS} should be determined to minimize biomass consumption. Meanwhile, the design capacity of heat recovery system C_{HR} and heat exchanger C_{HX} are determined by the design capacity of power generation unit $C_{PGU,e}$. To save computational time while represent the year-round performance, the winter week with the highest heating load and the summer week with the highest cooling load is chosen as the objective function. Due to the relatively higher solar radiation, the electrical power production from BIPV and PVT is higher in summer than that in winter. Therefore, $C_{PGU,e}$, C_B, C_{ES}, C_{HS}, C_{HR} and C_{HX} are determined to minimize the biomass consumption of the chosen winter week, while C_{AC}, C_{EC} and C_{CS} are determined to minimize the biomass consumption of the chosen summer week.

3.1.2 Optimization objective function

In winter, biomass is consumed by both the PGU and boiler to generate electrical and heating energy:

$$\min m_{b,winter} = \sum_{j=1}^{j=24\times 7} (m_{b,PGU,j} + m_{b,B,j}) \tag{1}$$

In summer, owing to the lower heating demand, boiler is turned off. Therefore, biomass is only consumed by the PGU, and

$$\min m_{b,summer} = \sum_{j=1}^{j=24\times 7} (m_{b,PGU,j}) \tag{2}$$

3.1.3 Optimization constraints

The optimization constraints of $C_{PGU,e}$, C_B, C_{AC}, C_{EC} are set that they do not exceed the maximum electricity, heating and cooling energy demand, respectively. The upper bound of capacity of each energy device is set to avoid over-sizing and profligacy of resources.

$$0 \le C_{PGU,e} \le \max D_{e,b} \tag{3}$$
$$0 \le C_B \le \max D_h \tag{4}$$
$$0 \le C_{AC} \le \max D_c \tag{5}$$
$$0 \le C_{EC} \le \max D_c \tag{6}$$

Meanwhile, C_{ES}, C_{HS} and C_{CS} are set that they are less than half-day electricity, heating and cooling energy produced by PGU, biomass boiler, absorption chiller and electric chiller, respectively.

$$0 \le C_{ES} \le 12\, C_{PGU,e} \tag{7}$$
$$0 \le C_{HS} \le 12(C_{PGU,h} + C_B) \tag{8}$$
$$0 \le C_{CS} \le 12(C_{AC} + C_{EC}) \tag{9}$$

3.2 Second-stage optimization

Based on the optimal design capacity of energy devices determined from the first-stage optimization at each iteration, the objective of the second-stage optimization is to determine the operating capacity of energy devices in the MES to minimize its biomass consumption. It is expected that the electricity storage, the heating storage and the cooling storage can be fully utilized to shift the peak energy demands to off-peak periods.

3.2.1 Design variables

For winter period, the operating capacity of PGU $Q_{PGU,e}$, heat exchanger Q_{HX}, biomass boiler Q_B, charging rate of HS $r_{ch,HS}$, discharging rate of HS $r_{dch,HS}$, charging rate of ES $r_{ch,ES}$, discharging rate of ES $r_{dch,ES}$ are selected as the optimization variables at the second-stage optimization; For summer period, operating capacity of PGU $Q_{PGU,e}$, heat exchanger Q_{HX}, absorption chiller Q_{AC}, electric chiller Q_{EC}, charging rate of ES $r_{ch,ES}$, discharging rate of ES $r_{dch,ES}$, charging rate of CS $r_{ch,CS}$ and discharging rate of CS $r_{dch,CS}$ are chosen as optimization variables.

3.2.2 Objective function

The objective of the second-stage optimization is to minimize the weekly biomass consumption as set in Equations (1-2).

3.2.3 Optimization constraints

The optimization constraints include the balance between building energy demand and MES energy supply, as well as the operating constraints of the associated energy devices. Cooling, heating and electrical aspects of energy balance between the supply side (i.e. MES) and the demand side (i.e. commercial building) are summarized as follows:

$$D_c + r_{ch,CS} \leq Q_{AC} + Q_{EC} + r_{dch,CS} \tag{10}$$

$$D_h + r_{ch,HS} \leq Q_B + Q_{HX} + Q_{PVT,h} + r_{dch,HS} \tag{11}$$

$$D_e + Q_{PGU,e,CoC} + r_{ch,ES} \leq Q_{PGU,e} + Q_{BIPV} + Q_{PVT,e} + r_{dch,ES} \tag{12}$$

$$D_h = \begin{cases} D_{h,b} & in\ winter \\ D_{h,b} + Q_{HR\_AC} & in\ summer \end{cases} \tag{13}$$

$$D_e = \begin{cases} D_{e,b} & in\ winter \\ D_{e,b} + Q_{PGU\_EC} & in\ summer \end{cases} \tag{14}$$

The operating constraints of the energy devices are set follows: The operating capacity of the power generation unit, absorption chiller, electric chiller and biomass boiler should not surpass the corresponding design capacities determined at the first-stage optimization; energy stored in electricity and cold storage could not outstrip the respective design capacities:

$$0 \leq Q_{PGU,e} \leq C_{PGU,e} \tag{15}$$

$$0 \leq Q_{PGU\_HR} \leq C_{HR} \tag{16}$$

$$0 \leq Q_{HX} \leq C_{HX} \tag{17}$$

$$0 \leq Q_{AC} \leq C_{AC} \tag{18}$$

$$0 \leq Q_{EC} \leq C_{EC} \tag{19}$$

$E_{ES} \leq C_{ES}$ (20)

$E_{HS} \leq C_{HS}$ (21)

$E_{CS} \leq C_{CS}$ (22)

4. Results and discussion

In order to evaluate the performance of the proposed two-stage optimization approach, the performance of GA optimization is evaluated first. After that, the optimization results of design capacity and operating capacity are discussed to illustrate the performance of the proposed approach. Finally, the determined biomass consumption rate around the whole year is illustrated.

4.1 Performance evaluation of GA optimization

To prevent the optimization from being converged to local optimum, five different population size, five retain probabilities, four selection probabilities and four mutate probabilities are adopted in the two stages of optimization using the representative winter day. The optimization results are shown in Fig. 11. For each variable bar, the average value of other variables is obtained. For example, when calculating the bar value of *population size* = 20, the average value of 5 × 4 × 4 optimization results is adopted. Considering the computational time, the population size is set at 60 and 80 for first-stage and second-stage optimization, respectively. The retain probability, selection probability and mutation probability are chosen as 80%, 20%, and 20% for first-stage optimization, while 70%, 30% and 30% for second-stage optimization.

The two-stage capacity optimization approach is written in Python using the libraries of TensorFlow and Keras. The optimization program is running on the MacBook Pro with the processor of 2.9 GHz Intel Core i9. As summarized in Table 6, there are 60×80=4800 runs of GA optimization for the whole two stages, and it takes about 12 hours.

Table 6. Parameters for GA optimization.

	Optimization variables		Generations	Population size
	Winter	Summer		
First-stage	4	3	60	60
Second-stage	7×168	8×168	1000	80

The convergence performance of the chosen winter day and summer day is shown in Fig. 12. For the chosen winter day, the minimum weekly biomass consumption (2031 kg/week) is obtained after 37 and 692 iterations for the first-stage and second-stage optimization, respectively; For the chosen summer day, the optimal value of biomass consumption (257 kg/week) is obtained after 50 and 706 iterations for the first-stage and second-stage optimization, respectively.

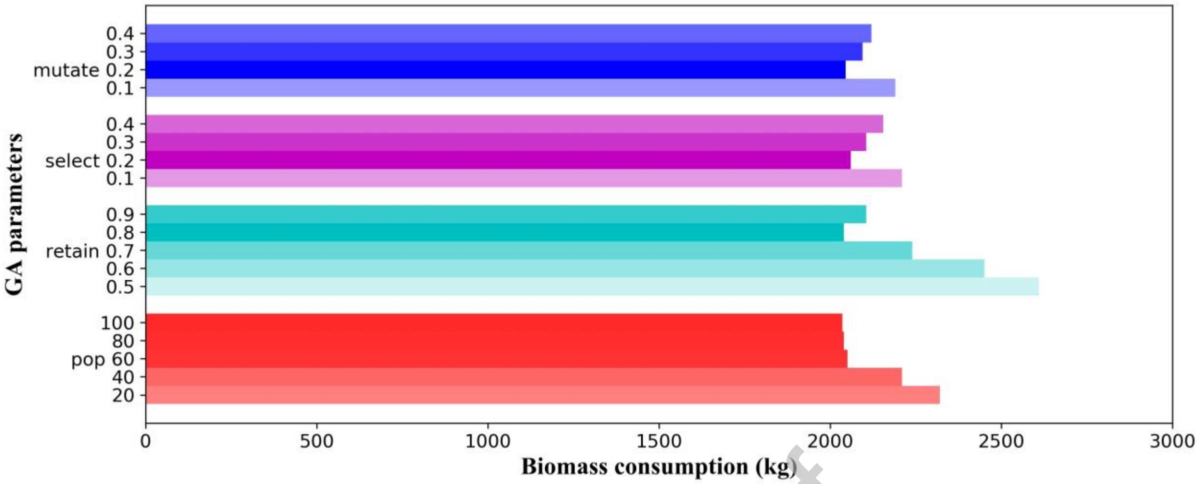

(a) First-stage optimization

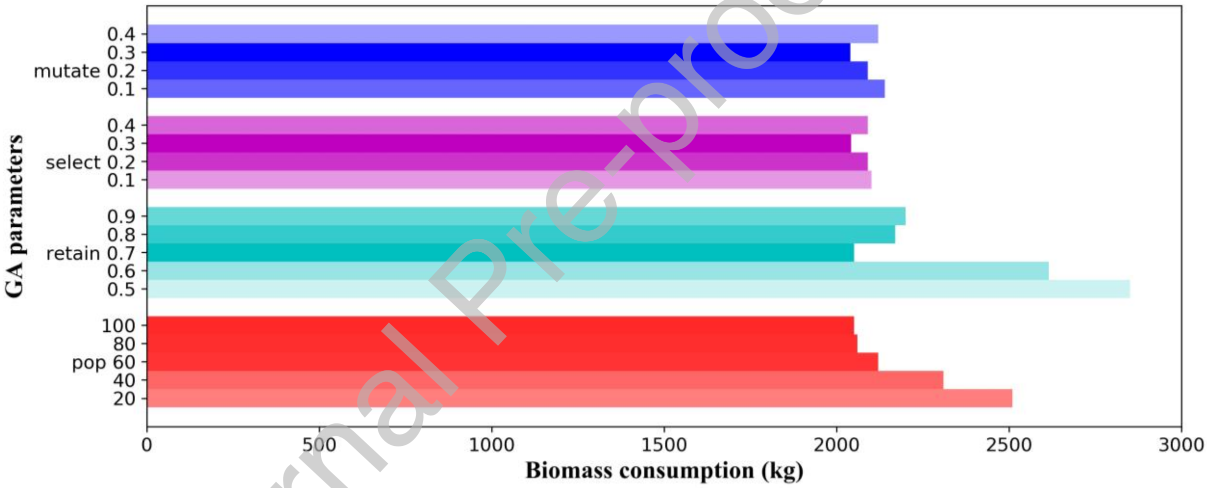

(b) Second-stage optimization

Fig. 11. Optimization results at different GA parameters.

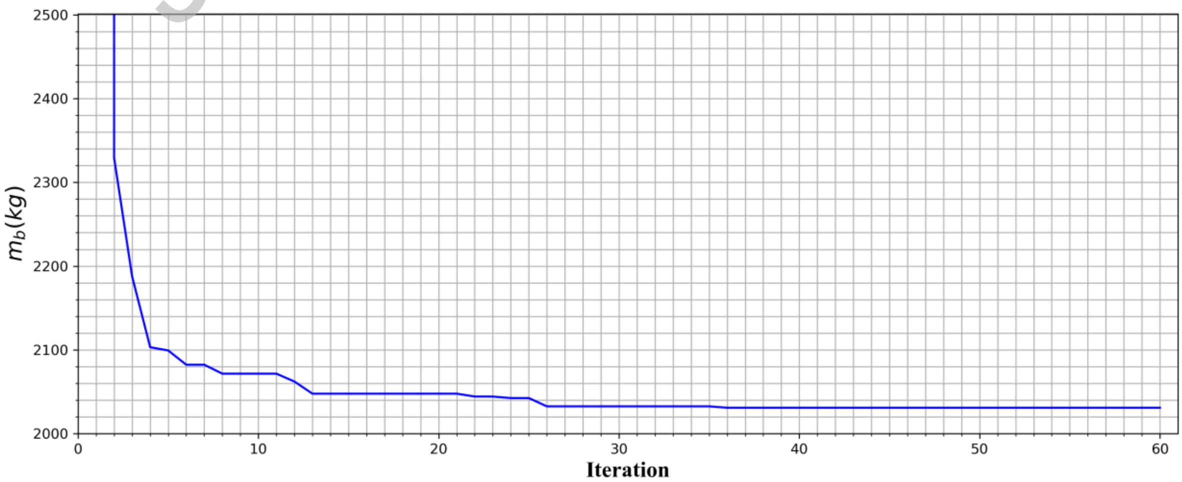

(a) First-stage optimization for winter day

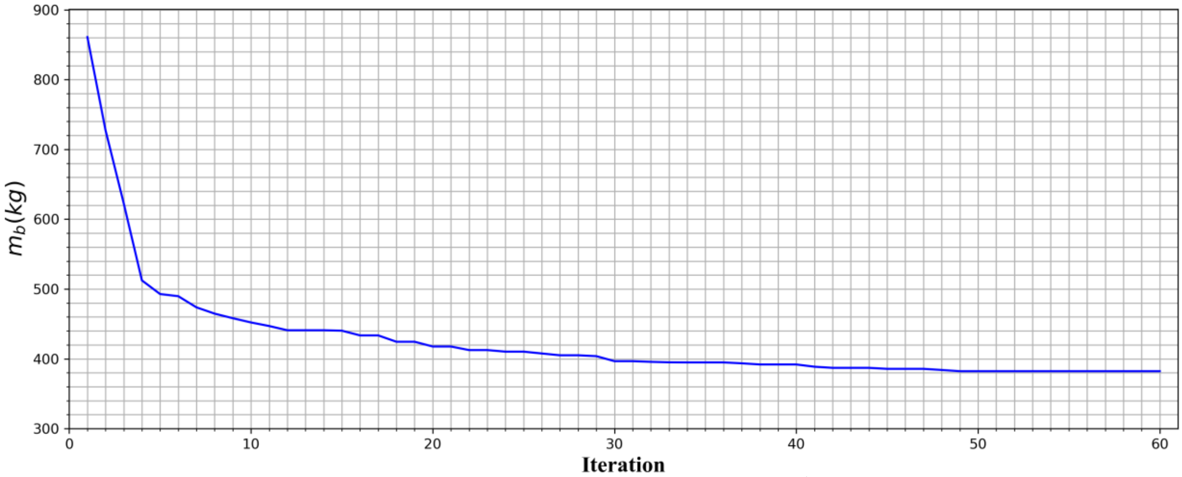

(b) First-stage optimization for summer day

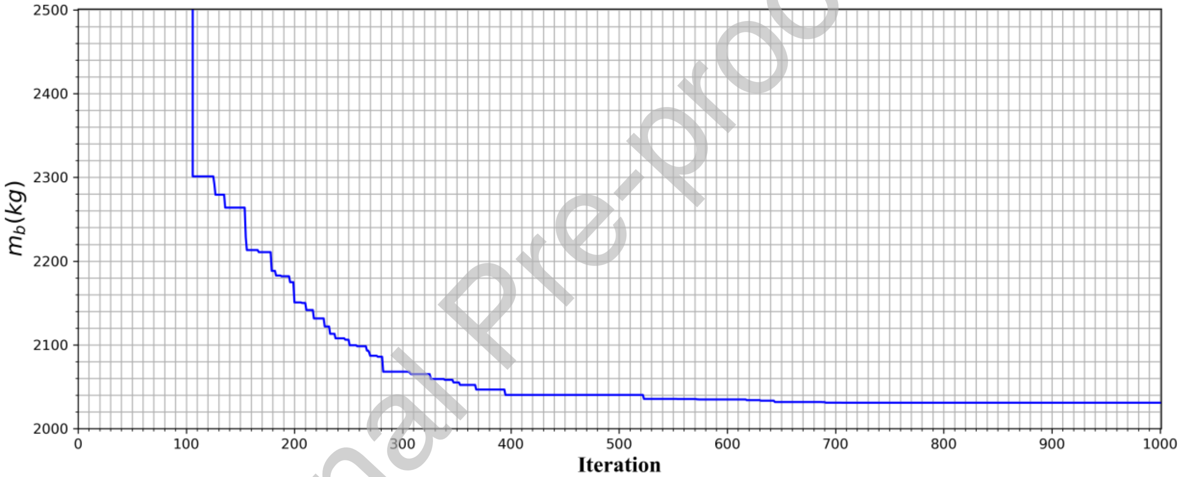

(c) Second-stage optimization for winter day

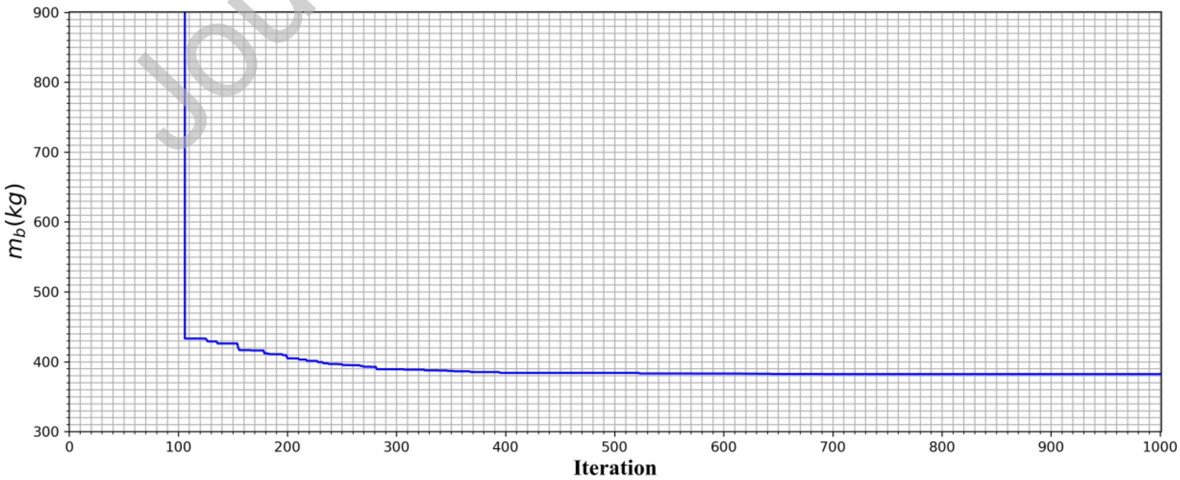

(d) Second-stage optimization for winter day

Fig. 12. Iteration performance of GA optimization.

4.2 *Optimization results of design capacities of energy devices*

To evaluate the performance of the proposed two-stage optimization approach, two reference cases were adopted as a comparison.

- To investigate the effectiveness of the operating capacity optimization at the second-stage, in the first reference case, following electricity load method is adopted in determining the operating capacity of each energy device in the first reference case, while GA optimization is adopted at first-stage for determining the optimal design capacity of energy devices: In winter, the operating capacity of PGU is determined according to the building electricity demand, while the boiler is operated when the thermal energy from PGU and PVT is not sufficient. In summer, the operating capacity of PGU is determined according to the building electricity demand, while the thermal energy recovered from PGU is firstly adopted for heating demand. The absorption chiller is driven by the thermal energy recovered from PGU and boiler. However, due to the limited capability of following electricity load method, electric chiller and energy storages are not adopted.
- To investigate the effectiveness of adopting the variable efficiency for PGU, absorption chiller and electric chiller, the proposed two-stage optimization approach is adopted in the second reference case while the efficiency of PGU, *COP* of absorption chiller and electric chiller is kept constant at 0.30, 0.78 and 6.5, respectively.

Through the proposed two-stage capacity optimization approach, the optimal design capacities of power generation unit $C_{PGU,e}$, biomass boiler C_B, absorption chiller C_{AC}, electric chiller C_{EC}, electricity storage C_{ES}, heating storage C_{HS} and cold storage C_{CS} can be determined. The optimization results are summarised in Table 7, along with the results from two reference caces. As discussed in Section 2.2, the peak heating, cooling and electricity demand is 464594, 306824 and 135190 kJ/h, respectively. Therefore, the optimization results from two-stage optimization approach indicate that the electrical energy from PGU is responsible for most of the peak electricity demand; biomass boiler is adopted for 86% of the peak heating demand; while absorption chiller and electric chiller takes up 74% and 27% of the peak cooling demand, respectively.

For both reference cases, the optimal design capacity of PGU, heat recovery unit and heat exchanger is the same as the two-stage optimization approach. For the first reference case, the design capacity of absorption chiller is kept the same as the peak cooling demand to guarantee the sufficient cooling energy supply. However, the design capacity of biomass boiler is a little smaller than that from the proposed two-stage optimization approach. For the second reference case, due to the assumed constant efficiency of each energy device, the design capacities of biomass boiler, absorption chiller, electric chiller, electricity storage, heat storage and cold storage are oversized.

Table 7. Optimization results of design capacity of energy devices

	Design capacity of energy devices (kJ/h)						(kJ)		
	$C_{PGU,e}$	C_{HR}	C_{HX}	C_B	C_{AC}	C_{EC}	C_{ES}	C_{HS}	C_{CS}
Proposed approach	135190	96891	77513	399940	227276	82259	911013	1020717	770000
Reference 1	135190	96891	77513	391090	306824				
Rereferenc 2	135190	96891	77513	494931	261010	82750	939512	1615826	831574

4.3 Optimization results of operating capacity of energy devices

After determining the optimal design capacity of energy devices through the proposed two-stage optimization approach, the year-round optimal operating capacity of each energy device is further determined using the second-stage optimization. The operating capacity of each energy device, along with the corresponding heating, cooling and electrical energy demand from one week in each month are summarized in Fig. 13.

From January to April and from October to the end of the year, basic heating energy demand refers to the thermal energy needed for both space heating and hot drinking water. During this period, PVT is used supply heating demand whenever there is enough solar radiation. Exhaust heat from PGU is also recovered through heat recovery system to provide thermal energy. However, the amount of recovered thermal energy depends on the part-load ratio of the PGU. If it is still not sufficient, biomass boiler would be operated to supplement the heating demand. Heat storage is also scheduled to charge when there is exceed heating supply while discharge when the thermal energy from PVT, PGU and biomass boiler is not sufficient.

- In January, February and December, the basic heating energy demand is relatively high while thermal energy production from PVT is relatively low, the biomass boiler is adopted to provide the large fraction of heating energy demand.
- In March and November, the basic heating energy demand is lower while the energy production from PVT is higher than that in January, February and December, the thermal energy supply from PVT, PGU and biomass boiler occupy similar fraction.
- In April and October, the basic heating energy demand is quite low, while the thermal energy from PVT and PGU is sufficient for heating energy supply. Therefore, biomass boiler is turned off while the extra thermal energy can be stored in the heat storage.

From May towards the end of September, basic heating energy is only needed for hot drinking water, which is much lower than that in other months. On the other hand, thermal energy recovered from

PVT is relatively high owing to the high solar radiation. As a result, thermal energy recovered from PVT is sufficient to supply the building basic heating energy demand. Meanwhile, the excessive thermal energy from PVT and PGU can be recovered to drive the absorption chiller for cooling purpose. Owing to the high solar radiation, thermal energy from PVT is much larger than that from PGU.

From January to April and from October to the end of the year, basic electrical energy demand refers to the building electricity for lighting and office equipment. The BIPV, PVT, PGU and electricity storage can be coordinated to satisfy the building electricity demand at any time of the period. When there is not sufficient daylight, artificial lighting is adopted, thus resulted in higher building electricity demand.

- In January, February, March, October, November and December, the electrical energy demand is relatively high while electricity energy production from BIPV and PVT is low. Therefore, the PGU is adopted to provide a large fraction of electrical energy demand.
- In April, the electrical energy production from BIPV and PVT is higher owing to the higher solar radiation. The BIPV, PVT and PGU share a similar amount of electrical energy production.

From May towards the end of September, the electrical energy includes the basic building electricity demand and the electricity consumption of the electric chiller. The BIPV, PVT and PGU share a similar amount of electrical energy production owing to the high solar radiation during this period. To keep the PGU working at the high part-load ratio, ES is charged when there is sufficient electricity supply. Meanwhile, ES is scheduled to be discharged during the night when the electricity demand is quite low and some of the daytime when necessary.

From May towards the end of September, cooling energy demand is needed due to high outdoor air dry-bulb temperature and solar radiation. It is seen from Fig. 13 that various cooling supply equipment units could work together to satisfy the cooling demand at any time on each day. Due to the large amount of thermal energy recovered from PVT and PGU, absorption chiller is scheduled to operate first. The electric chiller is scheduled to operate when there is sufficient electricity supply. Cooling storage would be charged when there is excessive cooling supply from absorption chiller while discharged to handle the cooling demand when necessary.

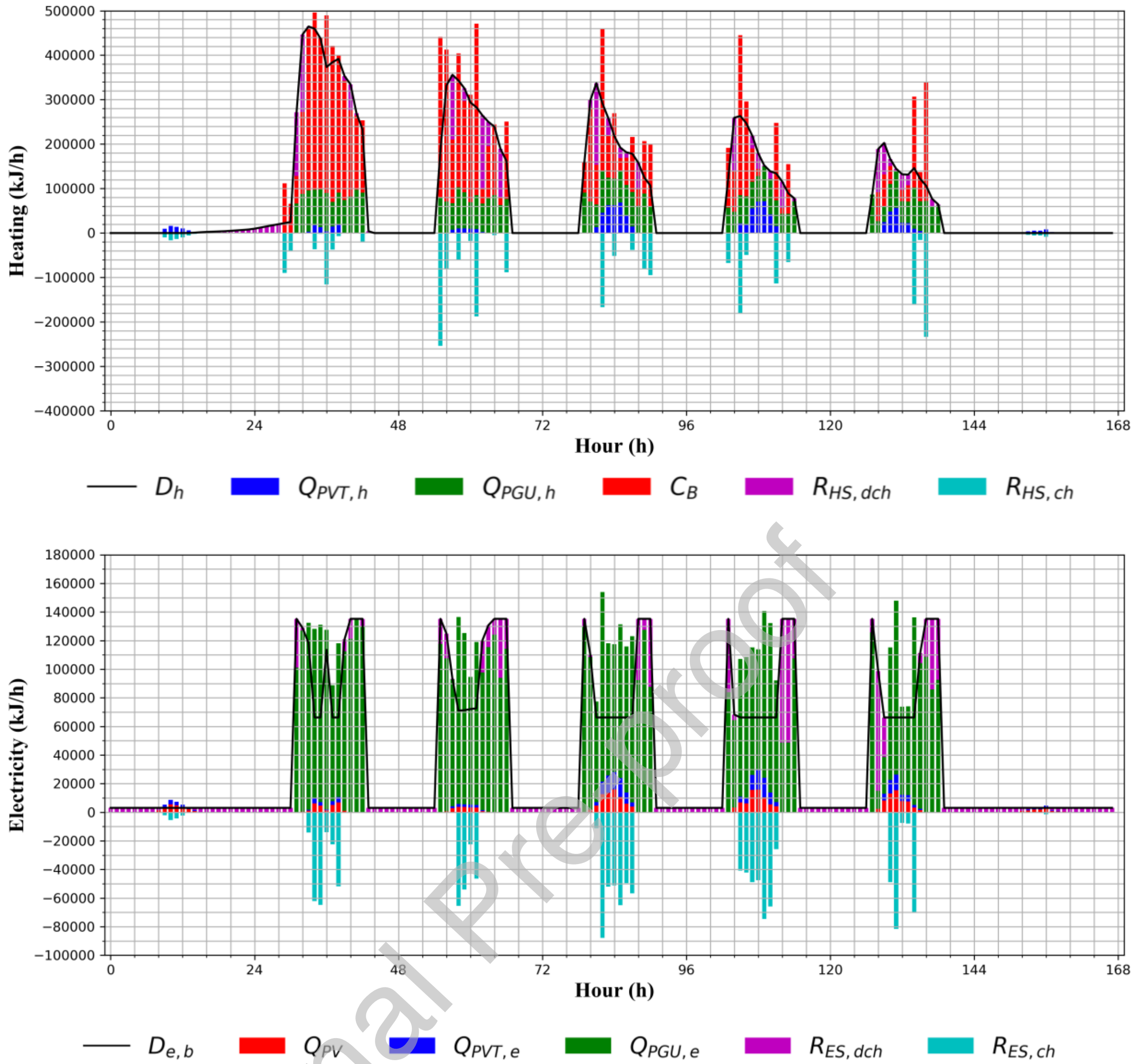
Heating (kJ/h)
Hour (h)
D_h $Q_{PVT,h}$ $Q_{PGU,h}$ C_B $R_{HS,dch}$ $R_{HS,ch}$
Electricity (kJ/h)
Hour (h)
$D_{e,b}$ Q_{PV} $Q_{PVT,e}$ $Q_{PGU,e}$ $R_{ES,dch}$ $R_{ES,ch}$

(a) January

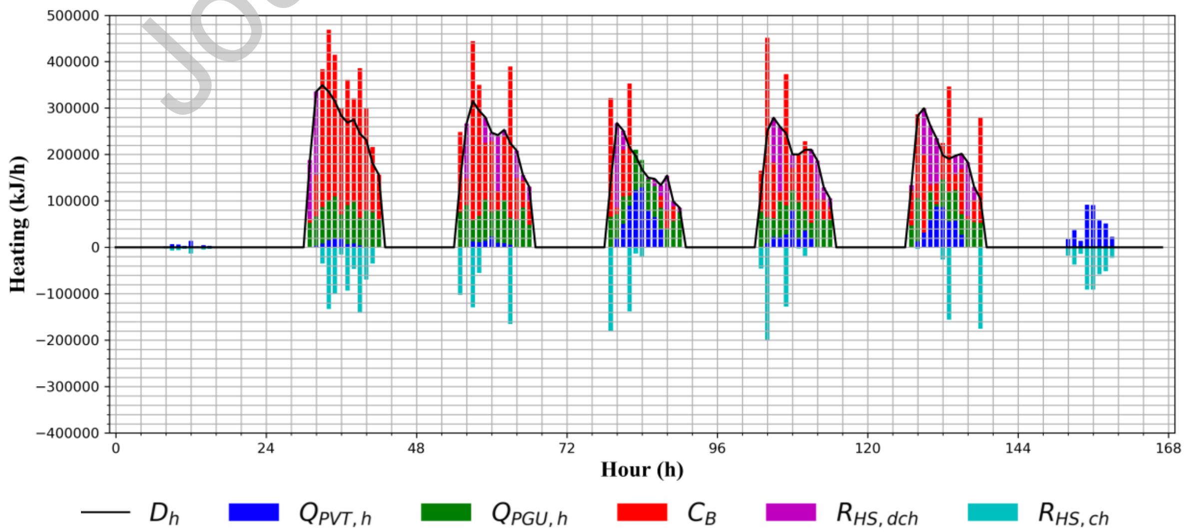
Heating (kJ/h)
Hour (h)
D_h $Q_{PVT,h}$ $Q_{PGU,h}$ C_B $R_{HS,dch}$ $R_{HS,ch}$

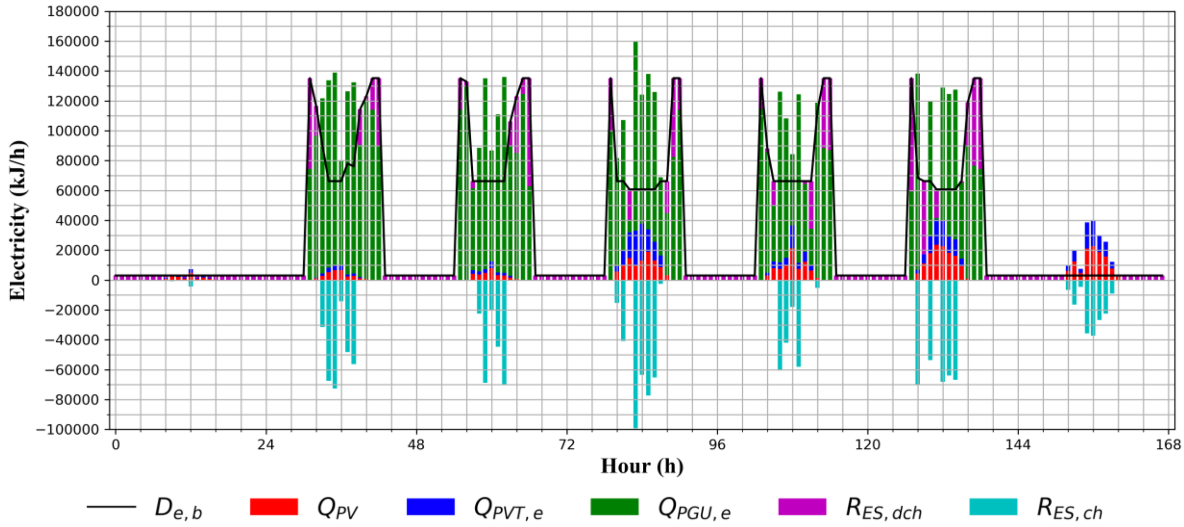

(b) February

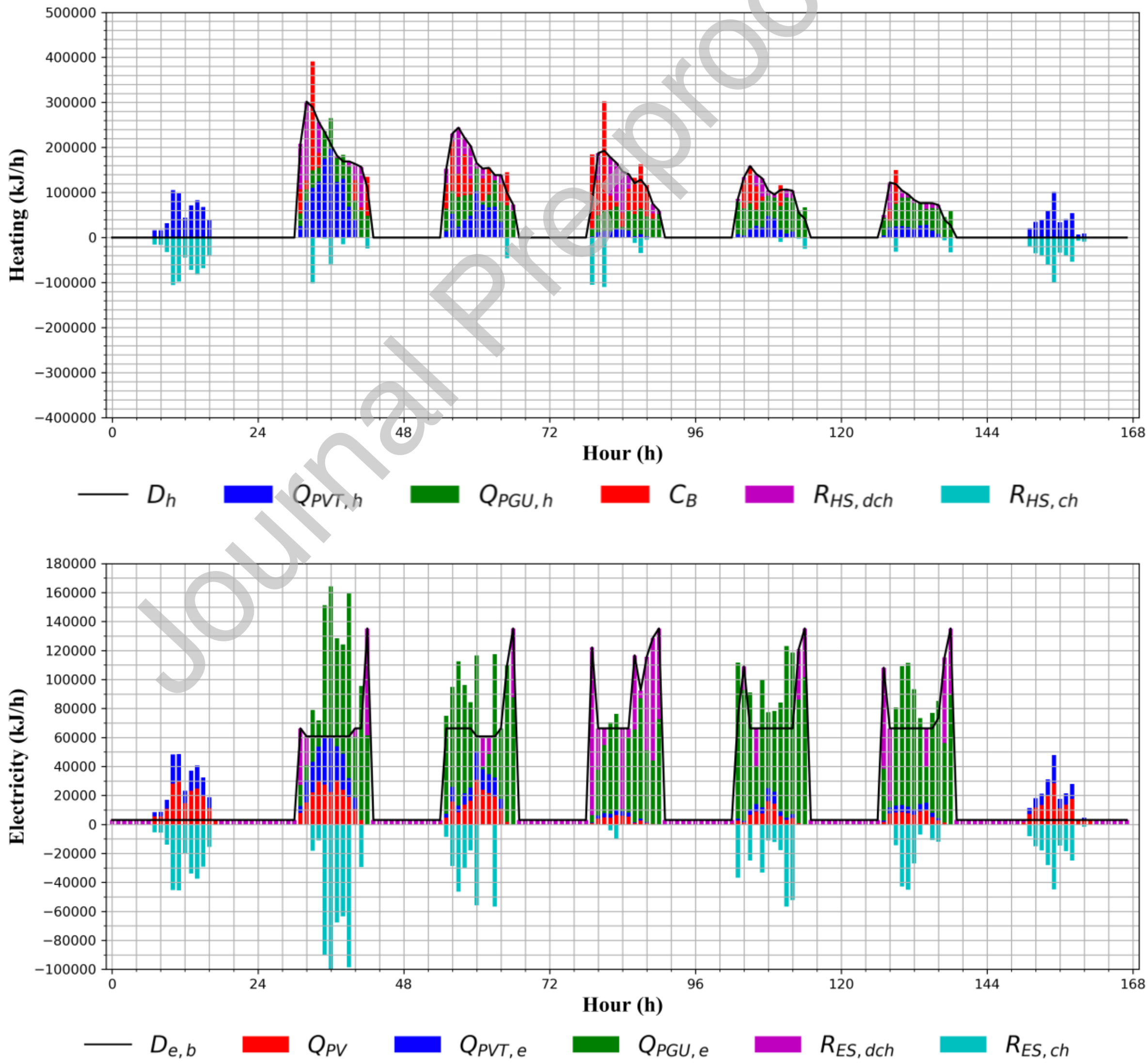

(c) March

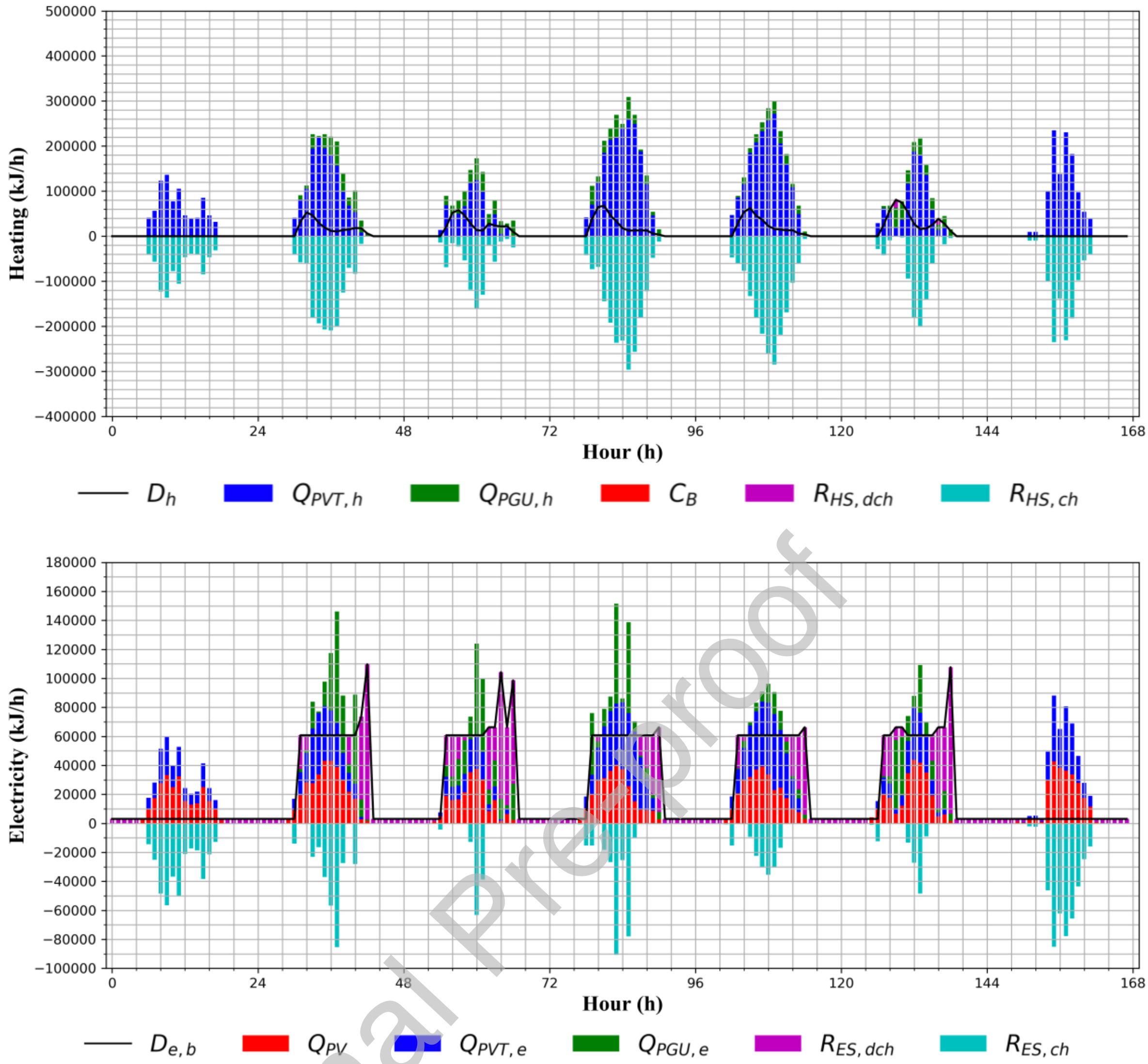
Heating (kJ/h)
500000
400000
300000
200000
100000
0
−100000
−200000
−300000
−400000
0
24
48
72
96
120
144
168
Hour (h)
D_h
$Q_{PVT,h}$
$Q_{PGU,h}$
C_B
$R_{HS,dch}$
$R_{HS,ch}$
Electricity (kJ/h)
180000
160000
140000
120000
100000
80000
60000
40000
20000
0
−20000
−40000
−60000
−80000
−100000
0
24
48
72
96
120
144
168
Hour (h)
$D_{e,b}$
Q_{PV}
$Q_{PVT,e}$
$Q_{PGU,e}$
$R_{ES,dch}$
$R_{ES,ch}$

(d) April

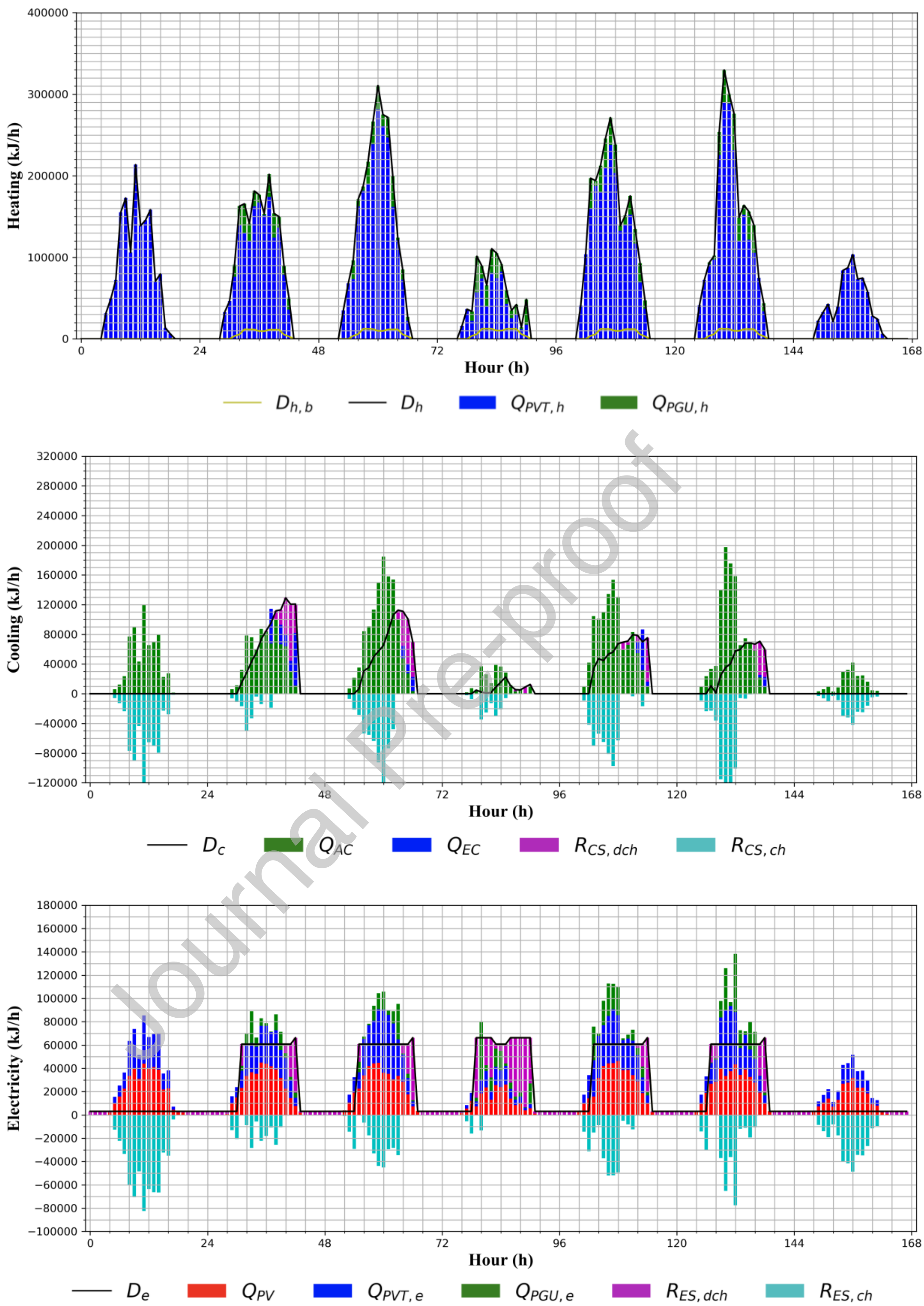
Heating (kJ/h)
Hour (h)
$D_{h,b}$
D_h
$Q_{PVT,h}$
$Q_{PGU,h}$
Cooling (kJ/h)
Hour (h)
D_c
Q_{AC}
Q_{EC}
$R_{CS,dch}$
$R_{CS,ch}$
Electricity (kJ/h)
Hour (h)
D_e
Q_{PV}
$Q_{PVT,e}$
$Q_{PGU,e}$
$R_{ES,dch}$
$R_{ES,ch}$

(e) May

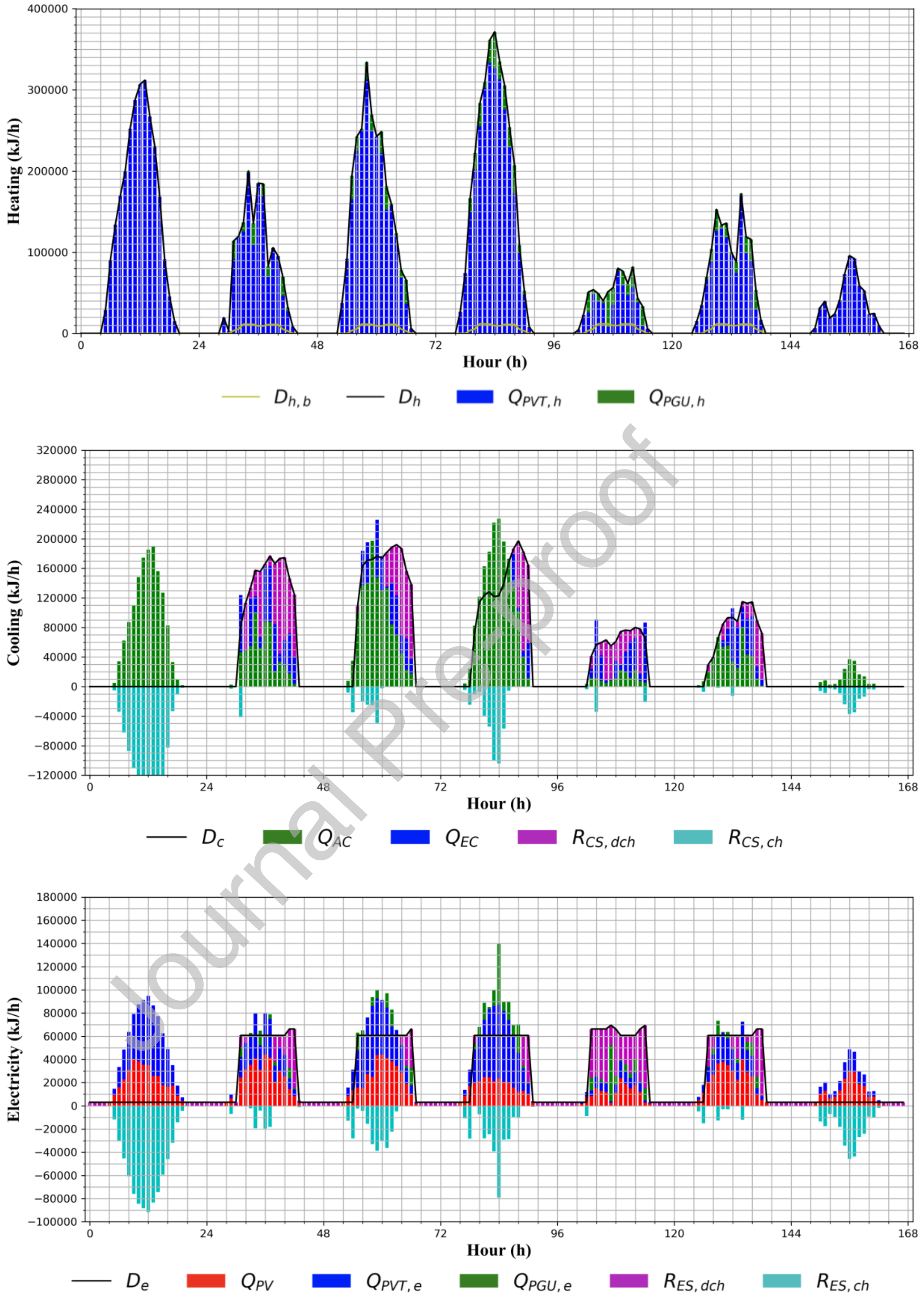

400000
300000
200000
100000
0
Heating (kJ/h)
0
24
48
72
96
120
144
168
Hour (h)
$D_{h,b}$
D_h
$Q_{PVT,h}$
$Q_{PGU,h}$
320000
280000
240000
200000
160000
120000
80000
40000
0
−40000
−80000
−120000
Cooling (kJ/h)
Hour (h)
D_c
Q_{AC}
Q_{EC}
$R_{CS,dch}$
$R_{CS,ch}$
180000
160000
140000
120000
100000
80000
60000
40000
20000
0
−20000
−40000
−60000
−80000
−100000
Electricity (kJ/h)
Hour (h)
D_e
Q_{PV}
$Q_{PVT,e}$
$Q_{PGU,e}$
$R_{ES,dch}$
$R_{ES,ch}$

(f) June

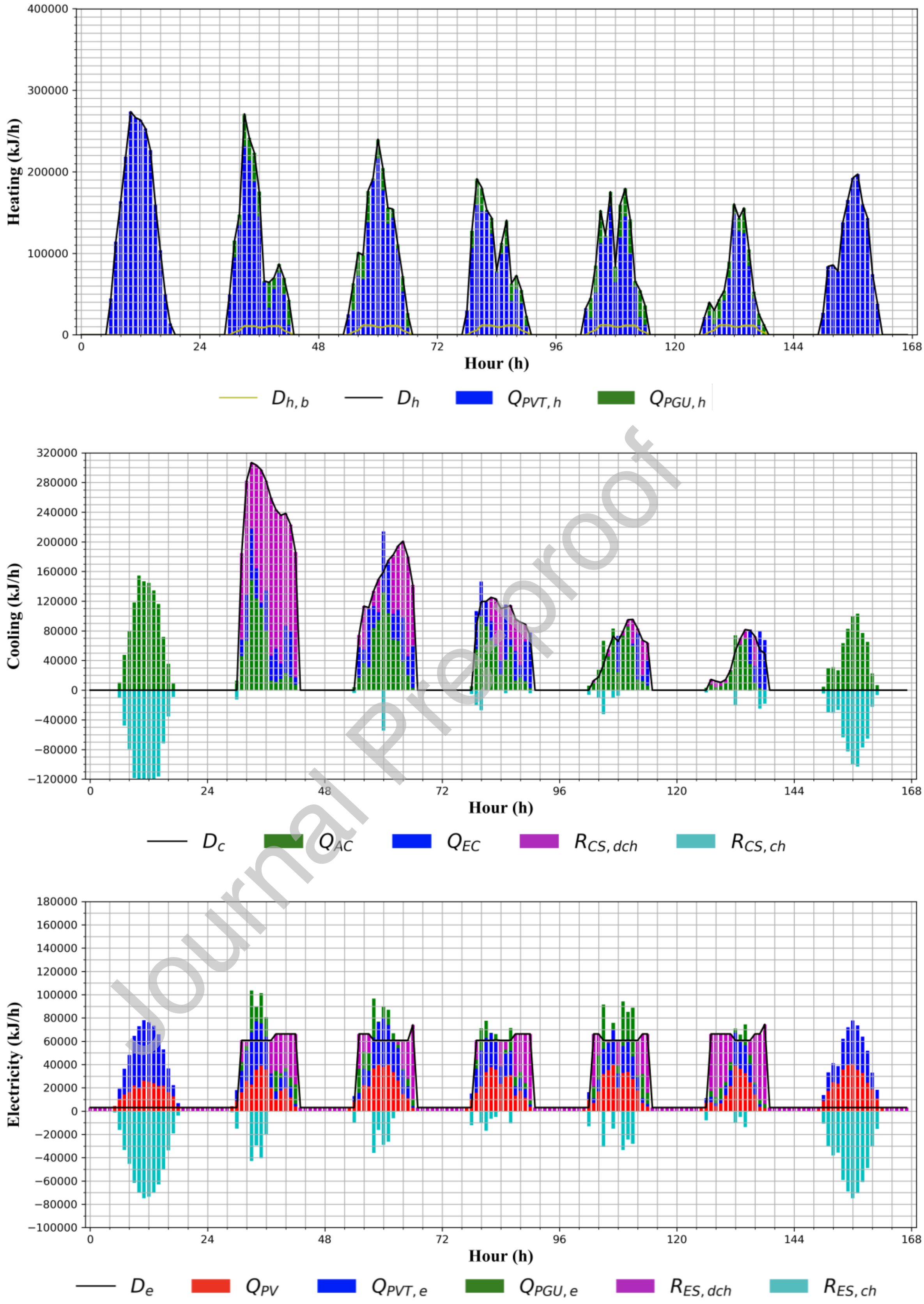

Heating (kJ/h)
Hour (h)
$D_{h,b}$
D_h
$Q_{PVT,h}$
$Q_{PGU,h}$
Cooling (kJ/h)
Hour (h)
D_c
Q_{AC}
Q_{EC}
$R_{CS,dch}$
$R_{CS,ch}$
Electricity (kJ/h)
Hour (h)
D_e
Q_{PV}
$Q_{PVT,e}$
$Q_{PGU,e}$
$R_{ES,dch}$
$R_{ES,ch}$

(g) July

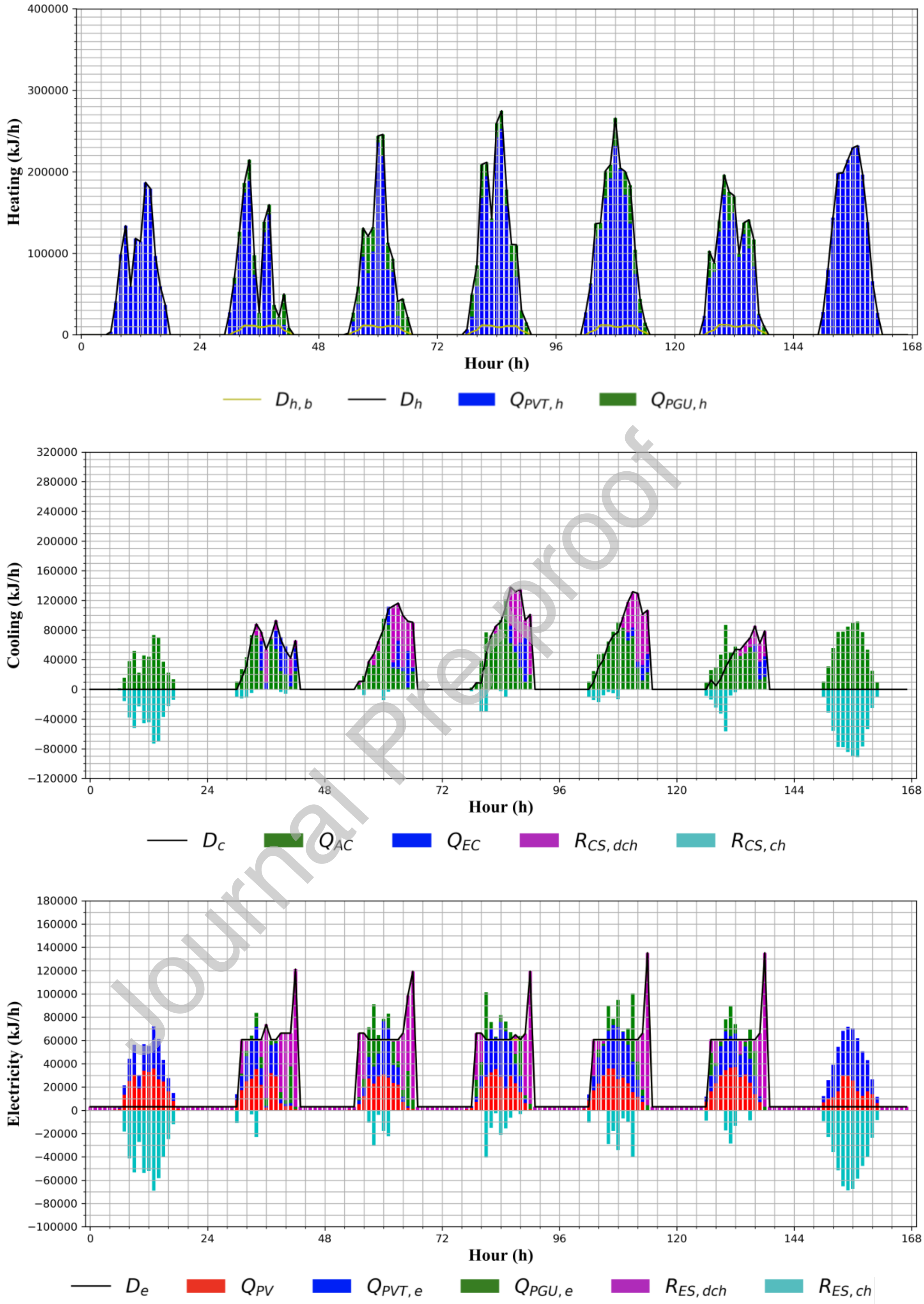

Heating (kJ/h)
Hour (h)
$D_{h,b}$
D_h
$Q_{PVT,h}$
$Q_{PGU,h}$
Cooling (kJ/h)
Hour (h)
D_c
Q_{AC}
Q_{EC}
$R_{CS,dch}$
$R_{CS,ch}$
Electricity (kJ/h)
Hour (h)
D_e
Q_{PV}
$Q_{PVT,e}$
$Q_{PGU,e}$
$R_{ES,dch}$
$R_{ES,ch}$

(h) August

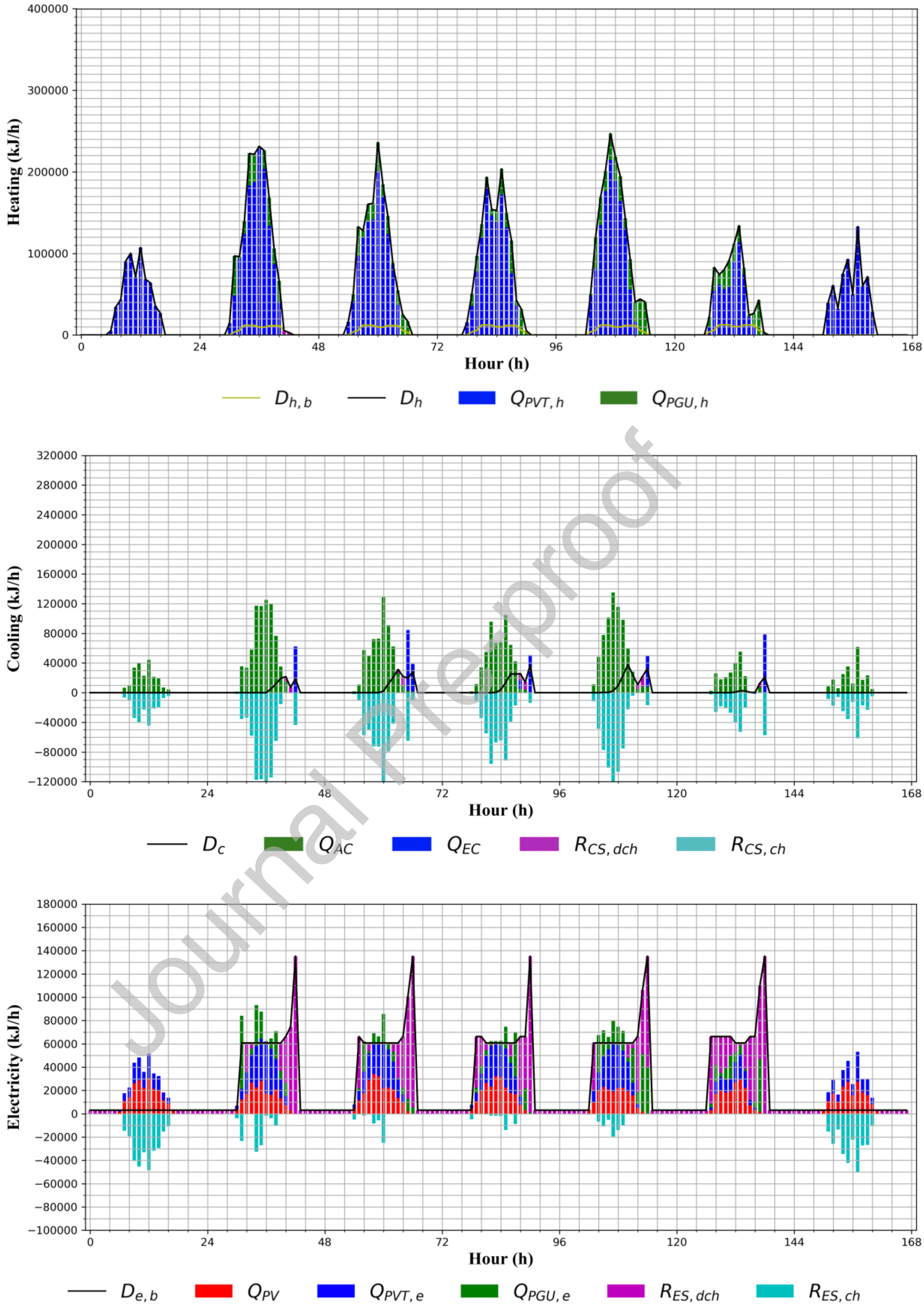
Heating (kJ/h)
400000
300000
200000
100000
0
0 24 48 72 96 120 144 168
Hour (h)
$D_{h,b}$
D_h
$Q_{PVT,h}$
$Q_{PGU,h}$
Cooling (kJ/h)
320000
280000
240000
200000
160000
120000
80000
40000
0
−40000
−80000
−120000
0 24 48 72 96 120 144 168
Hour (h)
D_c
Q_{AC}
Q_{EC}
$R_{CS,dch}$
$R_{CS,ch}$
Electricity (kJ/h)
180000
160000
140000
120000
100000
80000
60000
40000
20000
0
−20000
−40000
−60000
−80000
−100000
0 24 48 72 96 120 144 168
Hour (h)
$D_{e,b}$
Q_{PV}
$Q_{PVT,e}$
$Q_{PGU,e}$
$R_{ES,dch}$
$R_{ES,ch}$

(i) September

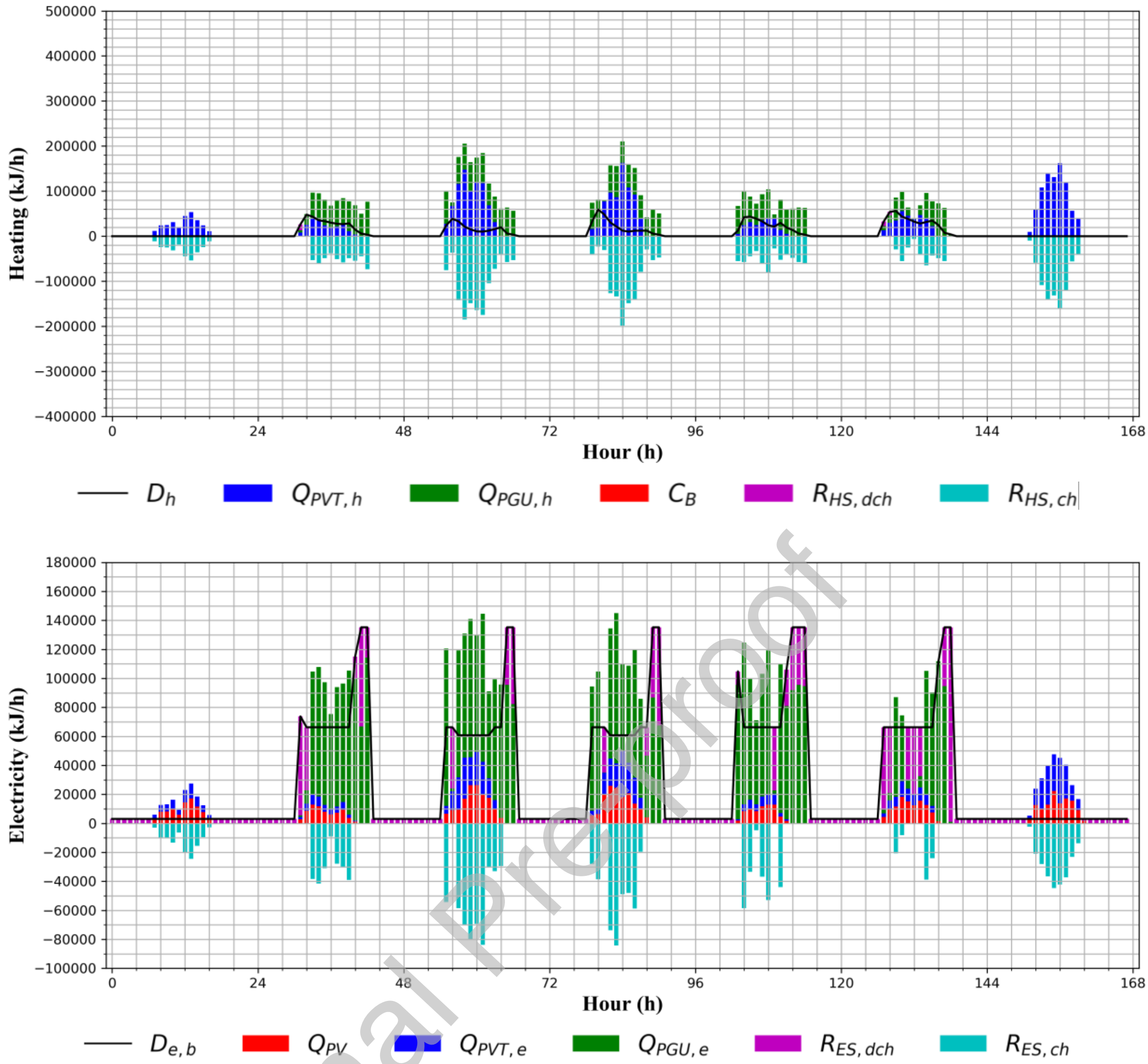

Heating (kJ/h)
500000
400000
300000
200000
100000
0
−100000
−200000
−300000
−400000
0
24
48
72
96
120
144
168
Hour (h)
D_h
$Q_{PVT,h}$
$Q_{PGU,h}$
C_B
$R_{HS,dch}$
$R_{HS,ch}$
Electricity (kJ/h)
180000
160000
140000
120000
100000
80000
60000
40000
20000
0
−20000
−40000
−60000
−80000
−100000
0
24
48
72
96
120
144
168
Hour (h)
$D_{e,b}$
Q_{PV}
$Q_{PVT,e}$
$Q_{PGU,e}$
$R_{ES,dch}$
$R_{ES,ch}$

(j) October

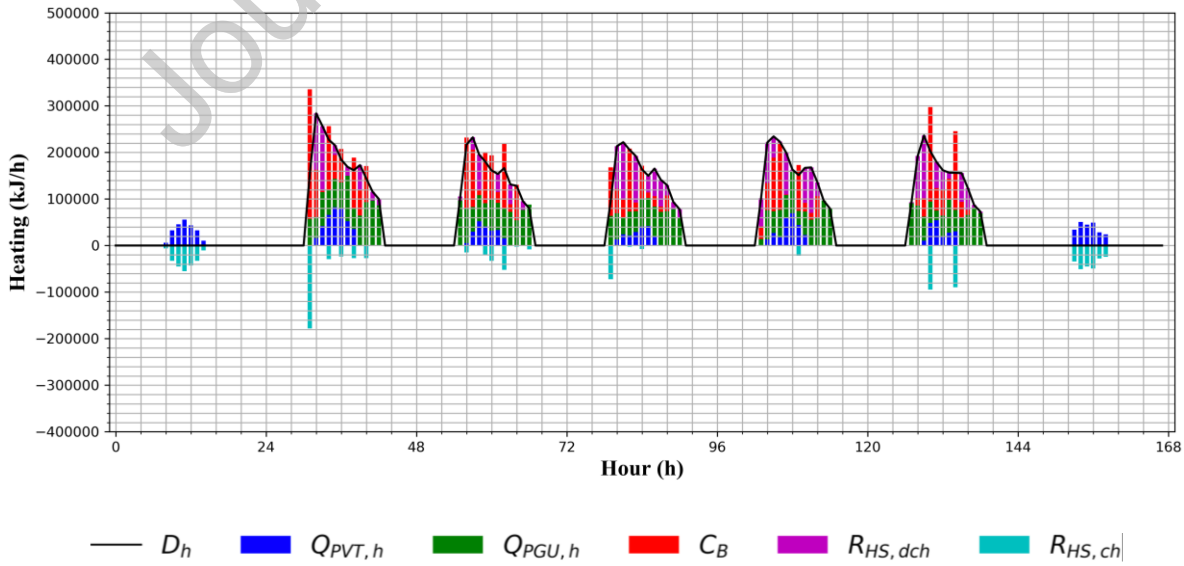

Heating (kJ/h)
500000
400000
300000
200000
100000
0
−100000
−200000
−300000
−400000
0
24
48
72
96
120
144
168
Hour (h)
D_h
$Q_{PVT,h}$
$Q_{PGU,h}$
C_B
$R_{HS,dch}$
$R_{HS,ch}$

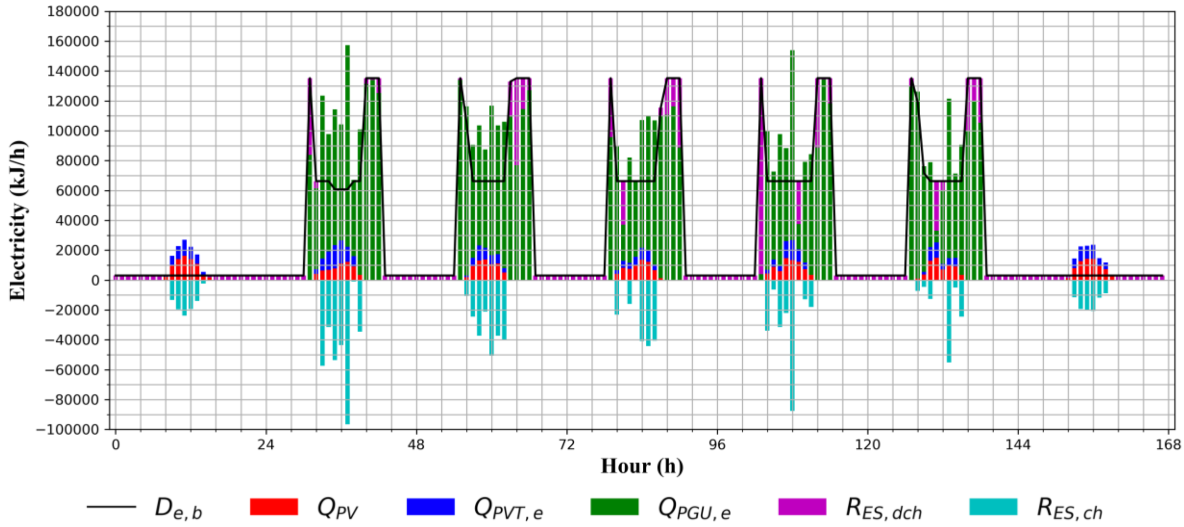

(k) November

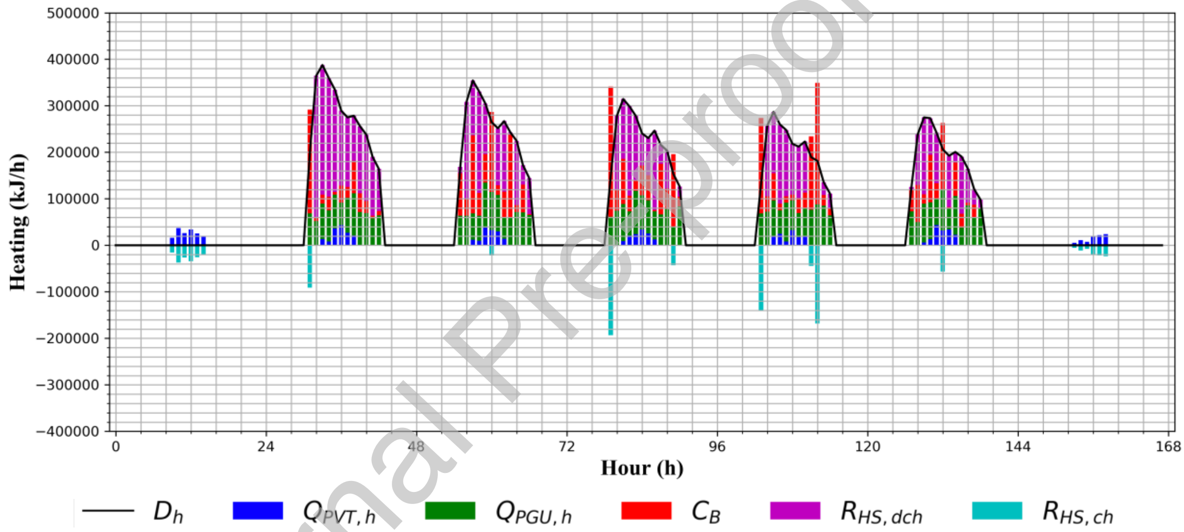

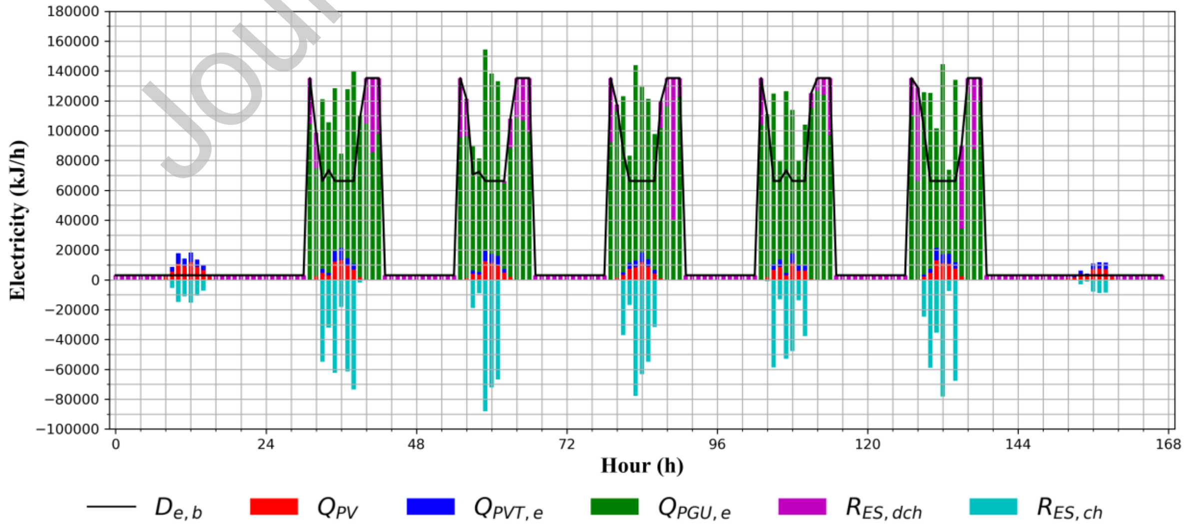

(l) December

Fig. 13. Operating capacity distribution of MES

4.4 *Performance evaluation of the biomass consumption*

The above-mentioned performance evaluation demonstrates that the proposed two-stage optimization approach can realize the effective and efficient design capacity optimization of the comprehensive MES. To further investigate the effectiveness of the proposed two-stage optimization approach, the biomass consumption from PGU and boiler is also assessed, as shown in Fig. 14. It is seen that the overall consumption of biomass by PGU is higher from January to April, as well as from August to December, while lower in other periods of the year. Because solar radiation is relatively higher from May to July, the higher electricity can be produced from BIPV and PVT thus PGU can be operated at a lower part-load ratio.

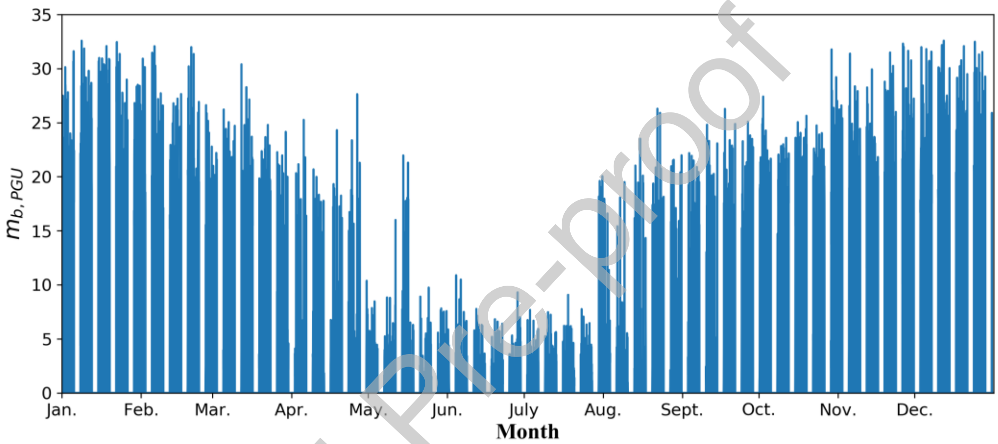

(a) PGU

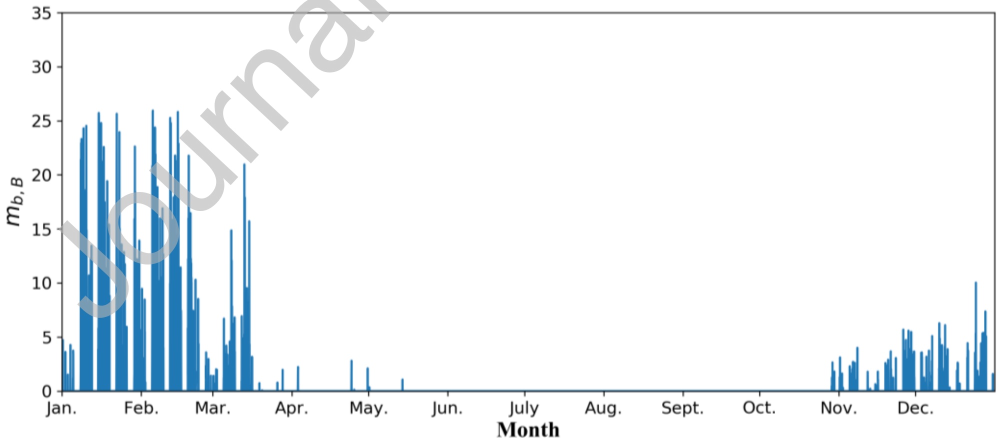

(b) Boiler

Fig. 14. Year-round biomass consumption

Meanwhile, the biomass consumption of boiler is higher from January to middle March, while lower during November and December. The heating demand is the highest in January and December. In November, the excessive thermal energy from the PGU can be stored in heat storage while being discharged to supplement the heating demand in December. From middle May to late October, the biomass boiler is scheduled to turn off owing to the low basic heating demand as discussed in Section 4.3.

The year-round biomass consumption resulted from the proposed two-stage optimization approach, reference case 1 and reference case 2 is 41977 kg, 48782 kg and 44960 kg, respectively. Therefore, the adoption of GA optimization in both first-stage (design) and second-stage (optimization) would result in 13.95% reduction of annual biomass consumption. The adoption of variable efficiency of key energy devices would lead to 6.63% reduction of year-round biomass consumption.

5. Conclusion

In this study, a two-stage capacity optimization approach is proposed for the comprehensive multi-energy system. The MES is driven by renewable energy while adopted to supply heating, cooling and electrical energy for a representative office. In the MES, solar energy is adopted in both BIPV and PVT for electricity production, in which the latter can generate thermal energy simultaneously. Biomass is delivered to gasification based PGU for electricity production. Meanwhile, both the exhaust heat from the PGU and the thermal energy from PVT can be recovered for heating purpose through the heat exchanger and cooling purpose through the absorption chiller. In addition, biomass is also delivered to boiler when the heating energy is not sufficient. When the cooling energy is not enough, the electricity generated by the PGU can be further utilized in electric chiller for cooling purpose. In addition, heat storage, cold storage and electricity storage are also adopted for different load shifting purposes.

The aim of the proposed optimization approach is to determine the optimal design capacity of each energy device involved in the MES. The biomass consumption during the winter week with the highest heating demand and during the summer week with the lowest cooling demand is chosen as the objective function in both the first-stage and second-stage optimization. The uniqueness of the proposed two-stage capacity optimization approach is summarized as below:

- The effectiveness of the proposed two-stage optimization approach is tested on a comprehensive MES, which consists of various energy devices, such as BIPV, PVT, biomass gasification based PGU, absorption chiller, electric chiller, heat exchanger, heat storage, cold storage and electricity storage.
- Since the optimal design capacity of each energy device is depended on its operating schedule, the optimal design capacity and operating capacity of the energy devices are obtained by performing two interrelated processes of optimization. The resulted optimal design capacity from the first-stage optimization is used as operational constraints in the second-stage optimization, while the resulted optimal operating capacity from the second-stage is adopted in determining the

objective function in the first-stage optimization. It is found that there is 13.95% reduction of the year-round biomass consumption compared to the design capacity optimization using conventional following electricity load strategy at the second-stage optimization.

- The variable efficiency of biomass gasification based PGU, absorption chiller and electric chiller at different loading and weather conditions is adopted to represent its practical performance. It is identified that there is 6.63% reduction of the annual biomass consumption compared to that with representative constant efficiency.
- To prevent the GA optimization from being converged to local optimum, the GA parameters, including population size, retain percentage, crossover percentage and mutation percentage are selected through enumeration method. The population size, retain probability, selection probability and mutation probability are chosen as 60, 80%, 20%, and 20% for the first-stage design capacity optimization, while 80, 70%, 30% and 30% for the second-stage operating capacity optimization.

In this study, the validated TRNSYS building thermal model is adopted to evaluate the heating, cooling and electrical energy demand of the representative office building. Meanwhile, the validated thermodynamic model of energy devices is adopted to simulate the performance of the MES. In practical application, the historical energy consumption and the operating performance of the existing building should be investigated to estimate its actual heating, cooling and electrical energy demand. Moreover, the actual operating data of the energy devices at different operating and weather conditions should be collected to calibrate the thermodynamic model. Based on the accurate thermal model of building and thermodynamic model of multiple energy devices, the proposed two-stage design capacity optimization approach can be used as an effective tool in building energy system retrofitting.

There are several directions for further refining the proposed two-stage capacity optimization approach:

- The effectiveness of the proposed two-stage capacity optimization approach should be tested on different types of buildings, such as the residential, hotel, restaurant and hospital buildings. Due to the different functions of the buildings, the characteristics of the heating, cooling and electrical energy demand would be different.
- To further guarantee the global optimal solution is identified by the GA optimization, other evolutionary optimization algorithms, including particle swarm optimization, ant colony optimization and artificial bee colony optimization, should be tested to see whether better optimal results can be identified.
- Biomass consumption is adopted as the single optimization function in the proposed two-stage capacity optimization approach. The energetic, economic and environmental life cycle

performance of the MES should also be investigated. Therefore, the proposed two-stage capacity optimization approach should be expanded to involve the multi-objective optimization.

1. Conflict of Interest

Potential conflict of interest exists:

We wish to draw the attention of the Editor to the following facts, which may be considered as potential conflicts of interest, and to significant financial contributions to this work:

The nature of potential conflict of interest is described below:

☒No conflict of interest exists.

We wish to confirm that there are no known conflicts of interest associated with this publication and there has been no significant financial support for this work that could have influenced its outcome.

2. Funding

☒Funding was received for this work.

All of the sources of funding for the work described in this publication are acknowledged below:

The Department for Business, Energy & Industrial Strategy (BEIS) through grant project number TEIF-101-7025.

☐No funding was received for this work.

3. Intellectual Property

☒We confirm that we have given due consideration to the protection of intellectual property associated with this work and that there are no impediments to publication, including the timing of publication, with respect to intellectual property. In so doing we confirm that we have followed the regulations of our institutions concerning intellectual property.

4. Research Ethics

☒We further confirm that any aspect of the work covered in this manuscript that has involved human patients has been conducted with the ethical approval of all relevant bodies and that such approvals are acknowledged within the manuscript.

☐IRB approval was obtained (required for studies and series of 3 or more cases)

☒Written consent to publish potentially identifying information, such as details or the case and photographs, was obtained from the patient(s) or their legal guardian(s).

5. Authorship

The International Committee of Medical Journal Editors (ICMJE) recommends that authorship be based on the following four criteria:

1. Substantial contributions to the conception or design of the work; or the acquisition, analysis, or interpretation of data for the work; AND
2. Drafting the work or revising it critically for important intellectual content; AND
3. Final approval of the version to be published; AND
4. Agreement to be accountable for all aspects of the work in ensuring that questions related to the accuracy or integrity of any part of the work are appropriately investigated and resolved.

All those designated as authors should meet all four criteria for authorship, and all who meet the four criteria should be identified as authors. For more information on authorship, please see http://www.icmje.org/recommendations/browse/roles-and-responsibilities/defining-the-role-of-authors-and-contributors.html#two.

☒All listed authors meet the ICMJE criteria. We attest that all authors contributed significantly to the creation of this manuscript, each having fulfilled criteria as established by the ICMJE.

☐One or more listed authors do(es) not meet the ICMJE criteria.

We believe these individuals should be listed as authors because:

☒We confirm that the manuscript has been read and approved by all named authors.

☒We confirm that the order of authors listed in the manuscript has been approved by all named authors.

6. Contact with the Editorial Office

The Corresponding Author declared on the title page of the manuscript is:

Lukumon Oyedele

☒This author submitted this manuscript using his/her account in EVISE.

☒We understand that this Corresponding Author is the sole contact for the Editorial process (including EVISE and direct communications with the office). He/she is responsible for communicating with the other authors about progress, submissions of revisions and final approval of proofs.

☒We confirm that the email address shown below is accessible by the Corresponding Author, is the address to which Corresponding Author's EVISE account is linked, and has been configured to accept email from the editorial office of American Journal of Ophthalmology Case Reports:

L.Oyedele@uwe.ac.uk

☐Someone other than the Corresponding Author declared above submitted this manuscript from his/her account in EVISE:

[Insert name below]

☐We understand that this author is the sole contact for the Editorial process (including EVISE and direct communications with the office). He/she is responsible for communicating with the other authors, including the Corresponding Author, about progress, submissions of revisions and final approval of proofs.

Acknowledgement

The authors would like to acknowledge and express their sincere gratitude to The Department for Business, Energy & Industrial Strategy (BEIS) through grant project number TEIF-101-7025. Opinions expressed and conclusions arrived at are those of the authors and are not to be attributed to BEIS.

Nomenclature

C	design capacity
COP	coefficient of performance
E	energy
LHV	lower heating value
m	consumption rate of biomass feedstock
PLR	part-load ratio
Q	operating capacity
r	charging/discharging rate
φ	solar radiation
η	efficiency

Subscripts

AC	absorption chiller
b	biomass
B	biomass boiler
BG	biomass gasification

c cooling
ch charging
CS cold storage
dch discharging
e electrical
EC electric chiller
ES electricity storage
ex exhaust
h heating
HR heat recovery system
HS heat storage
HX heat exchanger
j time step
MES multi-energy system
PGU power generation unit
PV building integrated photovaltic
PVT photovoltaic and thermal panel
rec recovery

Abbreviations

AC absorption chiller
BIPV building integrated photovoltaic
EC electric chiller
HX heat exchanger
ICE internal combustion engine
MES multi-energy system
PGU power generation unit
PVT photovoltaic thermal hybrid solar collector

References
[1] Luo XJ, Oyedele L, Ajayi A, Monyei C, Akinade O and Akanbi L. Development of an IoT-based big data platform for day-ahead prediction of building heating and cooling demands. Advanced Engineering Informatics, 41(2019)100926.
[2] Luo XJ and Fong KF. (2019). Investigation on part-load performances of combined cooling and power system primed by solid oxide fuel cell with different bottoming cycles. Journal of Power Sources, 429(2019)127-148.
[3] Luo XJ and Fong KF. Development of multi-supply-multi-demand control strategy for combined cooling, heating and power system primed with solid oxide fuel cell-gas turbine. Energy Conversion and Management, 154(2017)538-561.
[4] Luo XJ and Fong KF. Development of integrated demand and supply side management strategy of multi-energy system for residential building application. Applied Energy, 242(2019)570-587.
[5] Simeoni P, Nardin G and Ciotti G. 2018. Planning and design of sustainable smart multi energy systems. The case of a food industrial district in Italy. Energy, 163(2018)443-456.
[6] Wang JJ, Chen YZ and Noam L. Exergo-economic analysis method and optimization of a novel photovoltaic/thermal solar-assisted hybrid combined cooling, heating and power system. Energy Conversion and Management, 199(2019)111945.
[7] Luo ZY, Sheng Y, Nan X, Xie WW, Liu JX, Yawovi SA and Liu ZQ. Multi-objective capacity optimization of a distributed energy system considering economy, environment and energy. Energy Conversion and Management, 200(2019)112081.
[8] Pan GS, Wei G, Zhi W, Lu YP and Lu S. Optimal design and operation of multi-energy system with load aggregator considering nodal energy prices. Applied Energy, 239(2019)280-295.
[9] Wei F, Wu QH, Jing ZX, Chen JJ and Zhou XX. Optimal unit sizing for small-scale integrated energy systems using multi-objective interval optimization and evidential reasoning approach, Energy,111(2016)933-946.

[10]Zeng R, Li HQ, Liu LF, Zhang XF and Zhang GQ. A novel method based on multi-population genetic algorithm for CCHP–GSHP coupling system optimization. Energy Conversion and Management, 105(2015)1138-1148.
[11]Abdollahi G, and Hoseyn S. Application of the multi-objective optimization and risk analysis for the sizing of a residential small-scale CCHP system. Energy and Buildings, 60(2013)330-344.
[12]Li CY, Wu JY, Chavasint C, Sampattagul S, Kiatsiriroat T and Wang RZ. Multi-criteria optimization for a biomass gasification-integrated combined cooling, heating, and power system based on life-cycle assessment. Energy conversion and management, 178(2018)383-399.
[13]Lin HS, Yang CZ and Xu XQ. A new optimization model of CCHP system based on genetic algorithm. Sustainable Cities and Society, 52(2020)101811.
[14]Bahlawa H, Mirko M, Michele P, and Pier RS. Dynamic programming based methodology for the optimization of the sizing and operation of hybrid energy plants. Applied Thermal Engineering, (2019)113967.
[15]Wang Y, Li M, Hassanien RHE, Ma X and Li G. Grid-Connected semitransparent building-integrated photovoltaic system: The comprehensive case study of the 120 kWp Plant in Kunming, China. International Journal of Photoenergy, 2018.
[16]X.J. Luo. Development of dynamic model and control strategy of combined cooling, heating and power system primed with solid oxide fuel cell-gas turbine for building application. PhD thesis, City University of Hong Kong, 2018.
[17]Staffell I and Rustomji M. Maximising the value of electricity storage. Journal of Energy Storage, 8(2016)212-225.
[18]Compton M and Rezaie B. 2017. Sustainability Enhancement of a Biomass Boiler through Exergy Analysis. In Multidisciplinary Digital Publishing Institute Proceedings, 2(2017)159.
[19]Korolija I, Marjanovic HL and Zhang Y. UK office buildings archetypal model as methodological approach in development of regression models for predicting building energy consumption from heating and cooling demands. Energy and Building. 60(2013)152-162.
[20]Ciulla G, Brano VL and D'Amico A. Modelling relationship among energy demand, climate and office building features: a cluster analysis at European level. Applied Energy. 183(2016)1021-1034.
[21]TRNSYS 18: A Transient System Simulation Program. Solar Energy Laboratory University of Wisconsin, Madison, USA.

Graphical Abstract

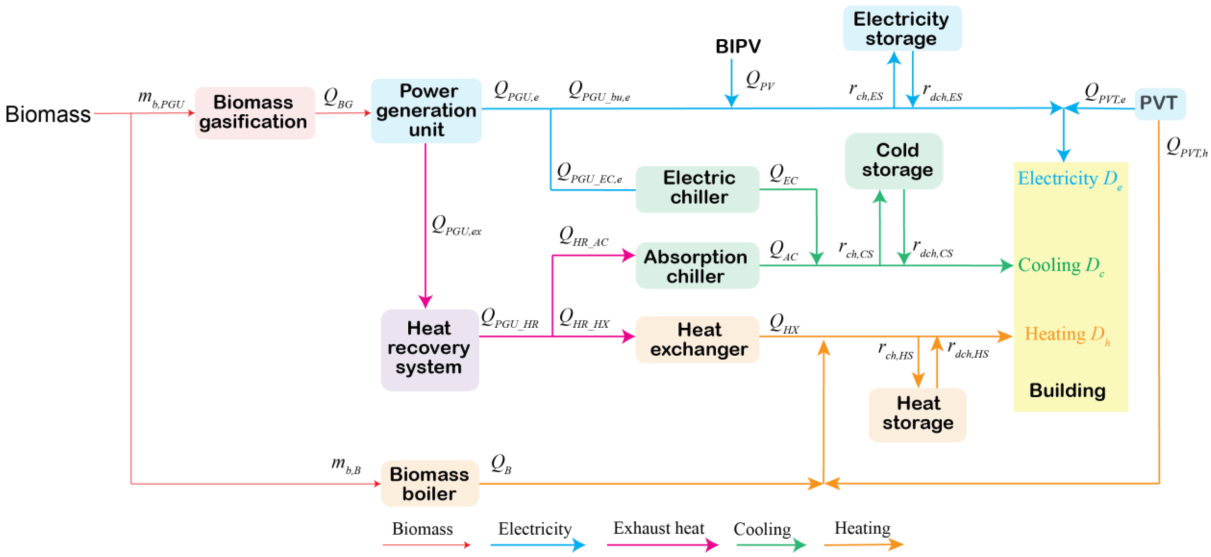

Multi-energy system

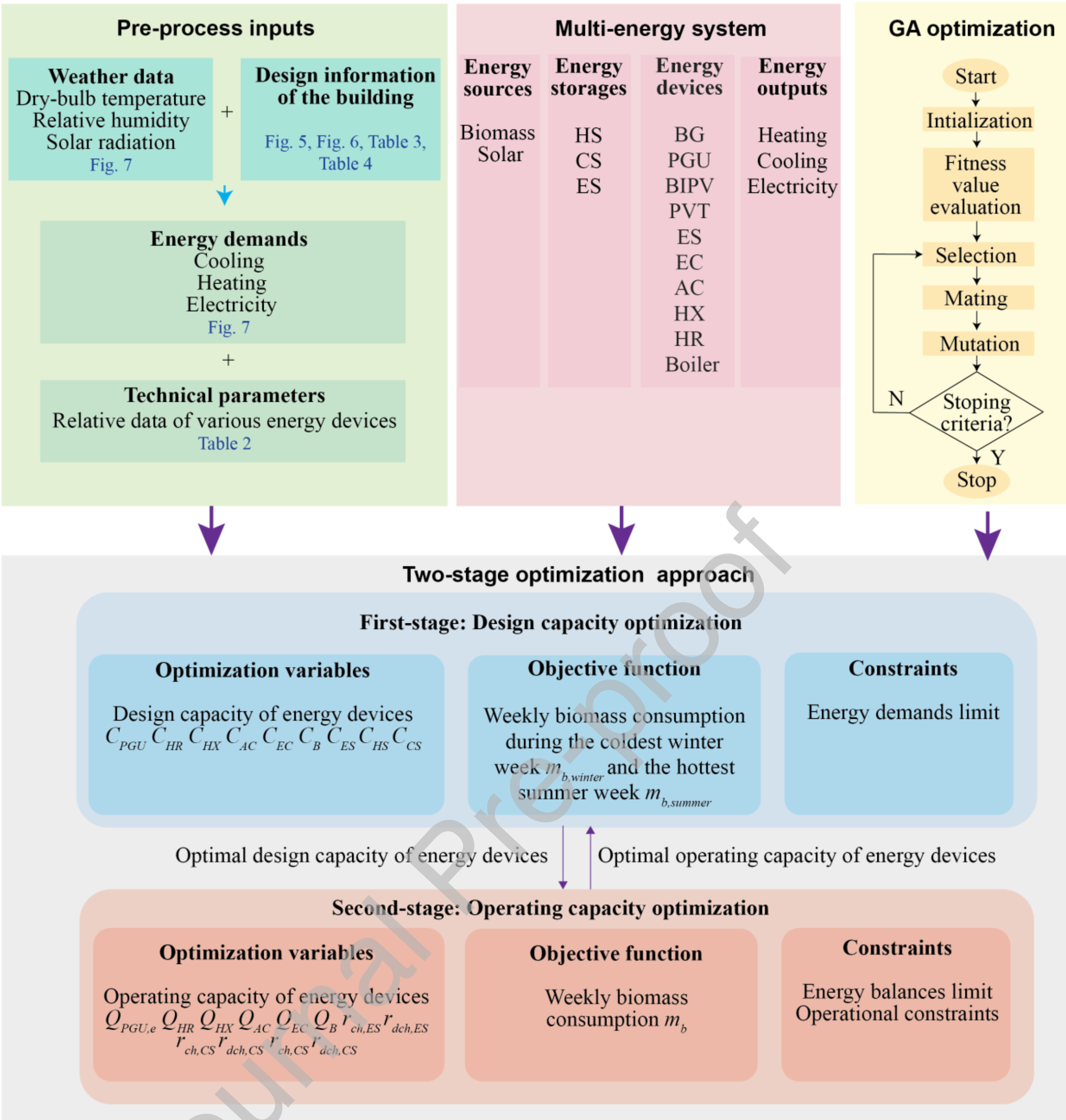

Two-stage optimization approach